



Citation for published version:

Zhen, L, Hu, Y, Wang, S, Laporte, G & Wu, Y 2019, 'Fleet deployment and demand fulfillment for container shipping liners', *Transportation Research Part B: Methodological*, vol. 120, pp. 15-32.
<https://doi.org/10.1016/j.trb.2018.11.011>

DOI:

[10.1016/j.trb.2018.11.011](https://doi.org/10.1016/j.trb.2018.11.011)

Publication date:

2019

Document Version

Peer reviewed version

[Link to publication](#)

Publisher Rights

CC BY-NC-ND

University of Bath

Alternative formats

If you require this document in an alternative format, please contact:
openaccess@bath.ac.uk

General rights

Copyright and moral rights for the publications made accessible in the public portal are retained by the authors and/or other copyright owners and it is a condition of accessing publications that users recognise and abide by the legal requirements associated with these rights.

Take down policy

If you believe that this document breaches copyright please contact us providing details, and we will remove access to the work immediately and investigate your claim.

1 Fleet deployment and demand fulfillment for container
 2 shipping liners

3 Lu Zhen^a, Yi Hu^a, Shuaian Wang^{b,*}, Gilbert Laporte^c, Yiwei Wu^a

4 ^a*School of Management, Shanghai University, Shanghai, China*

5 ^b*The Hong Kong Polytechnic University Shenzhen Research Institute, Nanshan District, Shenzhen,*
 6 *China*

7 *Department of Logistics & Maritime Studies, The Hong Kong Polytechnic University, Hung Hom,*
 8 *Hong Kong*

9 ^c*Department of Decision Sciences, HEC Montréal, Montréal, Canada*

10 **Abstract**

This paper models and solves a fleet deployment and demand fulfillment problem for container shipping liners with consideration of the potential overload risk of containers. Given the stochastic weights of transported containers, chance constraints are embedded in the model at the strategic level. Several realistic limiting factors such as the fleet size and the available berth and yard resources at the ports are also considered. A non-linear mixed integer programming (MIP) model is suggested to optimally determine the transportation demand fulfillment scale for each origin-destination pair, as well as the ship deployment plan along each route, with an objective incorporating revenue, fixed operation cost, fuel consumption cost, holding cost for transhipped containers, and extra berth and yard costs. Two efficient algorithms are then developed to solve the non-linear MIP model for different instance sizes. Numerical experiments based on real-world data are conducted to validate the effectiveness of the model and the algorithms. The results indicate the proposed methodology yields solutions with an optimality gap less than about 0.5%, and can solve realistic instances with 19 ports and four routes within about one hour.

11 *Keywords:* Demand fulfillment; fleet deployment; transshipment; port capacity;
 12 stochastic container weight.

*Corresponding author. lzhen@shu.edu.cn (L. Zhen), wangshuaian@gmail.com (S. Wang)

1. Introduction

Shipping liners play an important role in today's economy which is becoming increasingly global, and more operations are being outsourced and moved offshore (Fransoo and Lee, 2013). Shipping liners run weekly-serviced ship routes with fixed schedules to transport containers for customers. Each shipping company operates its own shipping network covering a number of routes (services) and ports. A shipping liner cannot usually fulfill all customer demands in a given container transportation market due to the limitations of its fleet size and of the available port resources (e.g., berths and yard space), and because of some other unforeseen factors (Zhen, 2015, 2016). The transportation demand is usually characterized by the number of containers that need to be transported between the origin-destination (OD) pairs of the shipping network. Given the data on the full-size market demand, a shipping liner needs to determine an economic fulfillment scale for each OD pair's transportation demand, as well as the number of ships deployed on each route of its shipping network so as to maximize its profit. This is an important strategic decision for the managers of shipping liners.

The above strategic level problem involves intertwined decisions as well as numerous complex factors. While it is easy to understand that the demand fulfillment scale is positively related to the number of deployed ships, the optimal allocation of the available ships along the routes is not a straightforward decision because of the different unit transportation fees among OD pairs, the different cost configurations among the routes, and the complex underlying relationship between the OD pairs and the routes. A liner may not always fulfill as much transportation demand as possible by using all its available ships because the port resources reserved for the liner in the shipping network are fixed. Moreover, several features proper to the ocean shipping industry must also be considered in this strategic level decision problem. For example, the number of ships deployed on a route affects the ships' speed on each leg of a route, which further influences fuel consumption and cost. These costs and the fixed operation costs of the deployed ships jointly constitute the bulk of the cost for a shipping liner. In addition, the ship schedule of each route (service) affects the containers' storage time at the transshipment hubs which connect the routes in the shipping network. The holding cost of the transshipped containers should therefore

45 also be taken into account. Finally, the potential overload risk of containers should not
46 be ignored since the weights of the transported containers are stochastic. Wang et al.
47 (2016) state that almost all the existing literature regards the weights of containers as
48 constants and few existing studies consider the problem of container overload. How-
49 ever, the potential overload risk of containers occurs frequently and has irreparable
50 consequences. Indeed, ship overload accidents account for 60 percent of accidents on
51 inland waterways and up to 70 percent in some areas. Therefore, studying the over-
52 load risk of containers is practical. For example, a shipping liner may promise a quota
53 of 1,000 twenty-foot equivalent units (TEUs) to a customer with respect to an OD
54 pair, but when the shipping liners make long term decisions on the demand fulfillment
55 scale, the cargo types and weights in the containers are unforeseen. For example, the
56 weights of 1,000 TEUs of plastic and of metal are significantly different. The overload
57 risk should therefore also be controlled.

58 This paper provides a comprehensive study of this complex decision problem.
59 Given a shipping network with multiple routes connected by transshipment hubs and
60 the transportation demand information, we propose a non-linear chance-constrained
61 mathematical integer program (MIP) to optimally determine the transportation de-
62 mand fulfillment scale for each OD pair, as well as the ship deployment plan along
63 each route in order to maximize the total profit, equal the revenue earned by fulfilling
64 the demand, minus four types of cost: the fixed operation cost of the deployed ships,
65 the fuel cost, the cost for storing transshipped containers at ports, and the cost of
66 using extra port resources. The chance constraints embedded in the model control
67 the potential overload risk resulting from random container weights. In addition to
68 the chance constraints, the model contains other non-linear components. Some new
69 techniques are suggested to linearize the model into a mixed integer second-order cone
70 programming (MISOCP) model that can be tractable for some commercial solvers
71 such as CPLEX.

72 The remainder of this paper is organized as follows. Section 2 provides an overview
73 of the related literature. Section 3 describes the problem. A mathematical model is
74 proposed in Section 4, followed by a linearization scheme in Section 5. Two heuristics
75 are developed to solve the model in Section 6. Section 7 reports the results of our
76 computational experiments. Closing remarks and conclusions follow in Section 8.

77 2. Related works

78 There exist numerous related studies on fleet deployment. Readers interested in
79 overviews can refer to Ronen (1993), Christiansen et al. (2004), Christiansen et al.
80 (2013), and Meng et al. (2014). At the strategic decision level, the fleet deployment
81 problem (FDP) consists of assigning available vessels to predetermined voyages
82 (Fagerholt et al., 2009) in order to maximize profit or minimize cost.

83 Several linear programming and mixed integer linear programming models for the
84 FDP have been put forward. Perakis and Jaramillo (1991) were the first to develop
85 a linear programming model for the FDP, which takes account of ship capacity, and
86 minimizes service frequency requirements as well as ship charter cost. However, this
87 model works with continuous decision variables for the allocation of ships to shipping
88 routes, instead of integer variables. To remedy this problem, Jaramillo and Perakis
89 (1991) proposed an integer programming model. Cho and Perakis (1996) formulated
90 a MIP model for the FDP, where the demand of containers between two given
91 ports can be served by any shipping route passing through the two ports. Powell
92 and Perkins (1997) extended the model of Jaramillo and Perakis (1991) by adding
93 ship lay-out costs to the objective function. Álvarez (2009) proposed a MIP formulation
94 for the integrated optimization of vessel routing and fleet deployment. Based
95 on previous works, Gelareh and Meng (2010) developed a MIP model for the FDP
96 in which speed is a decision variable, and investigated the problem of ship speed
97 optimization to obtain optimal sailing speeds through a non-linear model, which can
98 be approximated as a MIP model. This model was later improved by Wang et al.
99 (2011). Meng and Wang (2011) investigated a multi-period fleet planning and FDP
100 with a known container demand for each OD pair and each period. Meng and Wang
101 (2010) proposed a chance-constrained model for the FDP under uncertain demand,
102 but ignored transshipment activities. Because the speed of ships has an impact on
103 fuel consumption cost, Zacharioudakis et al. (2011) developed a practical methodology
104 that considers the effect of speed on fuel consumption for shipping companies
105 to solve FDPs. Andersson et al. (2015) put forward an integrated model to optimize
106 fleet deployment and sailing speed for RoRo shipping companies. Zheng et al. (2015)
107 set up a shipping network for liner shipping alliances, and proposed a model with
108 consideration of ship deployment, cargo allocation, and container routing. Xia et al.

109 (2015) developed a comprehensive model to simultaneously and optimally determine
110 ship deployment, sailing speed, and container allocation in order to maximize profit
111 at the strategic level. Zhao et al. (2016) designed a novel method of fleet deployment
112 based on risk evaluation so as to take advantage of resources for navigation and reduce
113 risks. Monemi and Gelareh (2017) provided an integrated model considering shipping
114 network design, FDP and empty container repositioning. The number of routes and
115 their design play an endogenous role in their problem. Wang et al. (2017) proposed
116 a two-stage stochastic programming model to optimally solve the FDP and compute
117 the sailing speeds with the consideration of market uncertainties. Some studies have
118 incorporated container transshipment in FDPs. Wang and Meng (2012) developed
119 an MIP model for the FDP in which containers can be transshipped at any port,
120 which was extended by Meng and Wang (2012) by adding transit time constraints.

121 There also exist some studies on FDPs that consider the uncertainties of liner ser-
122 vice schedule or container shipment demand. Wang and Meng (2012), Qi and Song
123 (2012) and Bell et al. (2011) considered uncertainty in the liner service schedule but
124 ignored uncertainty in container shipment demand. In order to tackle demand uncer-
125 tainty, Meng and Wang (2010) proposed a chance-constrained model, which extends
126 the deterministic FDP to a FDP under uncertainty. Meng et al. (2012) assumed that
127 the container shipment demand is a random variable, and hence formulated a two-
128 stage stochastic integer programming model, and developed an algorithm integrating
129 sample average approximation with a dual decomposition and Lagrangian relaxation
130 method. Wang et al. (2012) further extended the model of Meng et al. (2012) by
131 adding the expectation and variance of the cost in the objective function.

132 In conclusion, several related studies on the FDP have not taken transshipment
133 activities into account. Although some authors did consider these, they did not incor-
134 porate the demand fulfillment decision and the potential overload risk of containers
135 due to their stochastic weights. Moreover, some port resources such as berths and
136 yard space, which are crucial in maritime activities, have also been ignored. (Liu
137 et al., 2016) conducted an integrated planning of the berth allocation and the yard
138 allocation in container terminals.

139 Our paper proposes an integrated decision model that compounds ship fleet de-
140 ployment and demand fulfillment decisions by considering crucial factors such as
141 transshipment activities, the stochastic weight of containers, port resources, the

142 timetabling of ship visits at each port of call, and the demand fulfillment scale for
 143 each OD pair. There is no doubt that these factors complicate this already difficult
 144 fleet deployment and demand fulfillment problem. We propose a comprehensive mod-
 145 el and we develop some techniques to handle the complexity resulting from the chance
 146 constraints. We believe the problem features considered in our study are realistic and
 147 new with respect to previous research.

148 3. Problem description

149 We consider a shipping liner operating on a network containing a set R of container
 150 shipping routes (services), which cover a set P of ports. Figure 1 depicts a shipping
 151 network with four routes and 19 ports. Each ship route r is described as (port p_{r1} ,
 152 port p_{r2}, \dots , port p_{ri}, \dots , port p_{rN_r} , port p_{r1}), which implies that ship route r has N_r
 153 ports of call as well as N_r legs. Let leg i denote the voyage from port p_{ri} to port
 154 $p_{r,i+1}$, where $p_{r,N_r+1} = p_{r1}$. We denote by I_r the set of legs in ship route r . The
 155 details on the objective and key constraints considered in this study are provided in
 the following subsections.

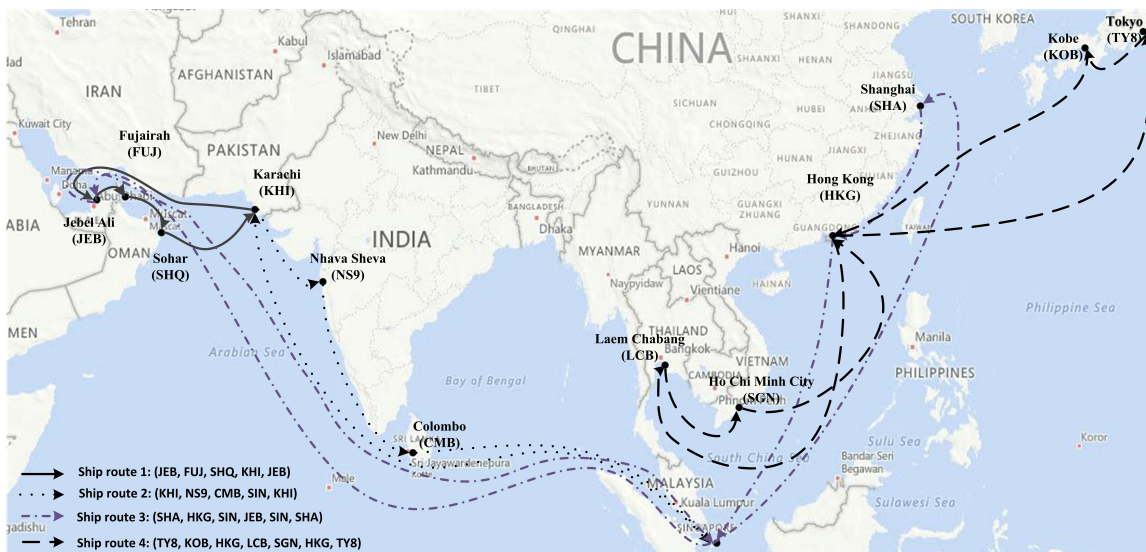


Figure 1: A shipping network with four routes

157 *3.1. Revenue of the demand fulfillment*

158 Container transportation demand is usually described by OD pairs indexed by
 159 $\varepsilon \in \Omega$. The number of containers requesting transport for each OD pair during a
 160 week can be estimated according to historical data. Given the unit fee for transporting
 161 a TEU container, we can compute the maximum revenue V_ε that can be earned if all
 162 the transportation demand of OD pair ε is fulfilled. We define a variable π_ε equal to
 163 the percentage of OD pair ε 's transportation demand fulfilled by the shipping liner.
 164 Then the total revenue can be calculated as $\sum_{\varepsilon \in \Omega} V_\varepsilon \pi_\varepsilon$.

165 *3.2. Fixed operation cost of deployed ships*

166 A fleet of homogeneous ships is deployed on each route to maintain a weekly
 167 service frequency. If the number of ships deployed on route r is β_r , then the total
 168 fixed operation cost for all the deployed ships in all the routes during one week can
 169 be calculated as $\sum_{r \in R} C_r^{Opr} \beta_r$, where C_r^{Opr} is the weekly operation cost for deploying
 170 one ship on route r .

171 *3.3. Fuel cost depending on sailing speed*

172 The total time for a ship completing the travel along a route is $7\beta_r$ days. More
 173 specifically, $\sum_{i \in I_r} (d_{ri} + \delta_{ri}) = 7\beta_r$, where d_{ri} is the dwell time of ships at the i^{th}
 174 port of call on ship route r , and δ_{ri} is the sailing time of ships on the i^{th} leg on ship
 175 route r . In reality, the port dwell time d_{ri} is usually predetermined according to some
 176 contracts between the shipping liner and port operators, but the sailing time δ_{ri} of
 177 each leg can be a decision variable for the shipping liner, which can be used to modify
 178 the value of δ_{ri} by updating the ships' speed on each leg.

179 A ship's unit fuel consumption significantly depends on its sailing speed. In this
 180 study, we assume that the unit fuel consumption function on sailing speed y is cal-
 181 culated as $y = kx^a$ (USD per nautical mile), where x is the speed, and k and a are
 182 positive coefficients. More specifically, the fuel cost for the i^{th} leg on ship route r is
 183 $l_{ri} k_{ri} (l_{ri} / \delta_{ri})^{a_{ri}}$, where l_{ri} is the leg's length, and k_{ri} and a_{ri} are coefficients that can
 184 be estimated according to historical data. The total fuel cost is then calculated as
 185 $\sum_{r \in R} \sum_{i \in I_r} l_{ri} k_{ri} (l_{ri} / \delta_{ri})^{a_{ri}}$.

186 *3.4. Holding cost for storing transshipped containers*

187 The above decisions on ship deployment and sailing speeds influence the cost
 188 related to each route which are inter-route costs. Decisions made on the arrival time
 189 of ships at each port of call in each route affect the storing time and cost of the
 190 containers at transshipment hubs, which are inter-route costs.

191 We define a quadruple (r, i, s, j) to denote that the i^{th} port of call on ship route
 192 r and the j^{th} port of call on ship route s are the same physical port in the network,
 193 where $r, s \in R, i \in I_r$ and $j \in I_s$. Hence $Q = \{(r, i, s, j) | p_{ri} = p_{sj}\}$. Let $m_{risj\varepsilon}$ be
 194 the maximum number of TEUs transshipped at hub (r, i, s, j) for OD pair ε if all
 195 the transportation demand for the OD pair is fulfilled. Then the number of trans-
 196 shipped containers at the hub is $\pi_\varepsilon m_{risj\varepsilon}$. We define a parameter C^{Hold} equal to the
 197 unit holding cost (USD per TEU per day), and a variable γ_{risj} to denote the dif-
 198 ference in days between the time a ship visits the port of call (r, i) and the time a
 199 ship visits (s, j) . Then the total holding cost for storing transshipped containers is
 200 $C^{Hold} \sum_{(r,i,s,j) \in Q} \sum_{\varepsilon \in \Omega} \pi_\varepsilon m_{risj\varepsilon} \gamma_{risj}$.

201 *3.5. Cost for using extra berth or yard space*

202 Each port has a certain yard space reserved for storing transshipped containers,
 203 and a certain number of berths for the shipping liner, booked in advance according
 204 to contracts. If the yard space and berth capacity limitations at ports are violated,
 205 then some extra costs are incurred (Petering et al., 2017).

206 In this study, we define B_p as the set of berths b in port p reserved for the shipping
 207 liner. Another index \hat{b} is defined as a dummy berth, which is used when there are no
 208 available berths in the reserved berth set B_p when a ship arrives at port p . From the
 209 perspective of modeling, if the dummy berth \hat{b} is used by a ship, then an extra cost
 210 is incurred. Here we define binary decision variables θ_{rib} to denote whether the ship
 211 arrives at berth b in the port of call (r, i) , and we define a parameter C_{pri}^{Berth} as the
 212 penalty cost incurred when the dummy berth \hat{b} is used in the port of call (r, i) . Then
 213 the total cost for extra berth usage is $\sum_{r \in R} \sum_{i \in I_r} C_{pri}^{Berth} \theta_{ri\hat{b}}$.

214 For the yard resource, we also define an auxiliary variable λ_{pw} as the extra used
 215 yard space (measured in number of TEUs) for storing transshipped containers at
 216 port p on day $w \in W$ of a week. The formula for computing the variable λ_{pw} will be

217 explained in the Section 4. Let C_p^{Yard} be the penalty cost for using one unit of extra
 218 yard space (TEUs), beyond the agreed reserved yard space, in port p to store the
 219 transshipped containers for one day. Then the total cost for extra yard space usage
 220 is $\sum_{p \in P} \sum_{w \in W} C_p^{Yard} \lambda_{pw}$.

221 3.6. Risk of overload due to random container weight

222 This study also considers the potential overload risk of ships due to the stochastic
 223 weight of transported containers. To illustrate this, suppose a liner promises a cus-
 224 tomer or an agency a quota of one thousand TEUs for an OD pair ε . When the liner
 225 makes the long term decision on the demand fulfillment scale for that OD pair, the
 226 weights of the cargos in the containers are unforeseen and may create an overload.
 227 We define a parameter $n_{ri\varepsilon}$ as the maximum number of containers transported on leg
 228 (r, i) for OD pair ε if all the transportation demand for the OD pair is fulfilled. Thus
 229 there will be $\lceil \pi_\varepsilon n_{ri\varepsilon} \rceil$ containers be transported on leg (r, i) for the OD pair ε . A
 230 stochastic parameter $\tilde{c}_{ri\varepsilon u}$ is defined as the random weight of the containers on leg
 231 (r, i) for OD pair ε , where u is the index of the container. Suppose the maximum
 232 load capacity (in tons) of a ship on leg (r, i) is A_{ri}^{Load} , and the probability of overload
 233 should be constrained to lie under a level α (e.g., 1%, 0.1%), then the constraint
 234 $\text{Prob}(\sum_{\varepsilon \in \Omega} \sum_{u=1}^{\lceil \pi_\varepsilon n_{ri\varepsilon} \rceil} \tilde{c}_{ri\varepsilon u} > A_{ri}^{Load}) \leq \alpha$ should hold for each leg (r, i) .

235 3.7. Assumptions and data preparation before using the model

236 Based on the above analysis on the revenue, on the various types of costs consid-
 237 ered in the objective function and on the chance constraints controlling the overload
 238 risk, we will formulate a mathematical model in the next section. We first clarify the
 239 assumptions of this study:

- 240 (1) the shipping network of the ports and routes (voyages) is already determined;
- 241 (2) the ships are homogenous on each route in terms of capacity and cost structure;
- 242 (3) the ships' dwell time at each port of call is deterministic.

243 Finally, we provide some explanation on how to prepare some key input data for
 244 the decision model. First, a shipping liner should collect the historical data on the
 245 weekly demand for each OD pair (Fagerholt et al., 2009; Bell et al., 2013). Based
 246 on the estimated unit price for shipping one TEU for each OD pair ε , the liner can
 247 calculate the V_ε values (i.e., the maximum revenue that can be earned if all the

248 transportation demand of the OD pair ε is fulfilled). Moreover, the mapping from
 249 an OD pair to a set of its covered legs as well as a set of transshipment ports is
 250 also deterministic. Given this mapping information, the liner can also estimate the
 251 parameters $n_{ri\varepsilon}$ (i.e., the maximum number of containers transported on each leg
 252 (r, i) for each OD pair ε) and the parameters $m_{risj\varepsilon}$ (i.e., the maximum number of
 253 containers transshipped from the port of call (r, i) to (s, j) for OD pair ε , if all the
 254 demand is fulfilled).

255 Another important input value is the stochastic parameter $\tilde{c}_{ri\varepsilon u}$ about the ran-
 256 dom container weight on the leg (r, i) for the OD pair ε . The liner could collect the
 257 historical data on the weights of containers transported for each OD pair ε , and then
 258 calibrate the expected value and standard deviation. Given the mapping information
 259 between an OD pair and the set of its covered legs, one can obtain the expected value
 260 $\mu_{ri\varepsilon}$ and the standard deviation $\sigma_{ri\varepsilon}$ for the random weights of containers transported
 261 on each leg (r, i) for each OD pair ε . These two parameters will be used in Section 5
 262 to linearize the chance constraints in the model.

263 4. Model formulation

264 We now introduce a non-linear chance-constrained MIP model for the problem.
 265 We first define some indices, sets, input parameters and decision variables.

266 Indices and sets

267	ε	index of an OD pair;
268	Ω	set of all the OD pairs;
269	r (or s)	index of a ship route;
270	R	set of all the ship routes;
271	i (or j)	index of port of call (or leg) on a ship route (leg i is from port of call i to $i+1$);
272	I_r	set of the ports of call (or legs) on ship route r ;
273	p	index of a physical port, which is different from the port of call (defined as i);

274	P	set of all the ports;
275	p_{ri}	index of the port, which corresponds to the port of call (r, i) ;
276	I'_{rp}	set of the ports of call (or legs) on ship route r ; these port of calls are the same physical port p ;
277	R'_p	set of ship routes that include port p ;
278	Q	set of quadruples (r, i, s, j) , where $r, s \in R; i \in I_r, j \in I_s$; a (r, i, s, j) means the ports of call (r, i) and (s, j) are the same physical port in shipping network. $Q = \{(r, i, s, j) p_{ri} = p_{sj}\}$;
279	Q_p	a subset of Q ; $Q_p = \{(r, i, s, j) p_{ri} = p_{sj} = p\}$;
280	w	index of a day in a week, i.e., $0 = \text{Sun}, 1 = \text{Mon}, 2 = \text{Tue}, \dots, 6 = \text{Sat}$;
281	W	set of days in a week, $W = \{0, 1, 2, \dots, 6\}$;
282	b	index of a berth;
283	B_p	set of berths in port p ; these berths are reserved for the shipping liner;
284	\hat{b}	index of a dummy berth, used when there are not available berths in the reserved berth set B_p when a ship arrives at port p ;
285	\mathbb{Z}	set of integers;
286	\mathbb{Z}_+	set of non-negative integers.
287	Parameters	
	V_ε	maximum revenue if all the transportation demand of OD pair ε is fulfilled;
288	$n_{ri\varepsilon}$	maximum number of containers (TEUs) transported on leg (r, i) for the OD pair ε if all the demand is fulfilled;
289	$m_{risj\varepsilon}$	maximum number of containers (TEUs) transshipped from the port of call (r, i) to (s, j) for the OD pair ε if all the demand is fulfilled; here $(r, i, s, j) \in Q$;
290	N_r^{Ship}	maximum number of ships that can be deployed on ship route r ;

291	T_{ri}^{Leg}	minimum sailing time on leg (r, i) , which is determined by ships' maximum speed;
292	A_p^{Port}	capacity (TEUs) of port p for storing the transshipped containers;
293	A_{ri}^{Vol}	maximum volume capacity (in TEUs) of a ship on leg (r, i) ;
294	A_{ri}^{Load}	maximum load capacity (in tons) of a ship on leg (r, i) ;
295	α	probability limit of overload risk for ships (e.g., 1%, 0.1%);
296	$\tilde{c}_{ri\epsilon u}$	stochastic parameter, the weight of the u^{th} container on the leg (r, i) for OD pair ϵ ;
297	$\mu_{ri\epsilon}$	the expected value for the random weight $\tilde{c}_{ri\epsilon u}$;
298	$\sigma_{ri\epsilon}$	the standard deviation for the random weight $\tilde{c}_{ri\epsilon u}$;
299	C_r^{Opr}	weekly operation cost of one ship deployed on ship route r ;
300	C^{Hold}	unit holding cost (USD per TEU per day) of transshipped containers storing at ports;
301	C_p^{Berth}	penalty cost each time the dummy berth \hat{b} is used at the port p ;
302	C_p^{Yard}	penalty cost for using one TEU extra yard space for transshipped containers in port p ;
303	d_{ri}	duration (days) of a ship dwells at the port of call (r, i) ;
304	\bar{D}	maximum value of d_{ri} for all the ports of call;
305	l_{ri}	length of the leg (r, i) ;
306	k_{ri}, a_{ri}	coefficients to calculate the unit fuel cost for travelling per nautical mile on leg (r, i) ;
307	g_{bw}	equals one if berth b is available on day w in a week, otherwise equals zero;

$f_{\dot{w}\ddot{w}}$ equals one if day w is in time interval from day \dot{w} to \ddot{w} ; otherwise equals zero. Here $\dot{w}, \ddot{w}, w \in W, W = \{0, 1, 2, \dots, 6\}$. For example, if $\dot{w} = 1, \ddot{w} = 3$, then $f_{\dot{w}\ddot{w}1} = f_{\dot{w}\ddot{w}2} = f_{\dot{w}\ddot{w}3} = 1$; if $\dot{w} = 3, \ddot{w} = 1$, then $f_{\dot{w}\ddot{w}3} = f_{\dot{w}\ddot{w}4} = f_{\dot{w}\ddot{w}5} = f_{\dot{w}\ddot{w}6} = f_{\dot{w}\ddot{w}0} = f_{\dot{w}\ddot{w}1} = 1$.

309 Decision variables

310 (1) Binary variables

311 η_{riw} binary variable equal to one if and only if the ship arrives at the port of call (r, i) on day w of a week;

312 θ_{rib} binary variable equal to one if and only if the ship uses berth b (including \hat{b}) in the port of call (r, i) .

313 (2) General integer variables

314 β_r number of ships deployed on ship route r ; here $\beta_r \in \{1, 2, 3, \dots, N_r^{Ship}\}$;

315 δ_{ri} sailing time (days) of leg (r, i) ;

316 τ_{ri} time (day) when a ship arrives at the port of call (r, i) , where $i = 1, 2, 3, \dots, |I_r| + 1$; $\tau_{r1} \in \{0, 1, 2, \dots, 6\}$; $\tau_{r, |I_r|+1}$ denotes the time at which the ship completes a round trip journey;

317 ζ_{ri} auxiliary variable associated with τ_{ri} , used to transform τ_{ri} into a day in one week;

318 γ_{risj} arrival time difference in days of a ship visiting (r, i) and a ship visiting (s, j) ;

319 ξ_{risj} auxiliary variable associated with γ_{risj} to transform γ_{risj} into an integer less than seven;

320 λ_{pw} extra used yard space (TEUs) for storing transshipped containers at port p on day w .

321 (3) Continuous variables

322 π_ε percentage of OD pair ε 's transportation demand fulfilled by the shipping liner.

323 **Mathematical model**

324 The model is then as follows:

$$\begin{aligned}
 [\mathbf{M1}] \text{ Maximize } Z = & \underbrace{\sum_{\varepsilon \in \Omega} V_\varepsilon \pi_\varepsilon}_{\text{Revenue}} - \underbrace{\sum_{r \in R} C_r^{Opr} \beta_r}_{\text{Ship operation cost}} - \underbrace{\sum_{r \in R} \sum_{i \in I_r} l_{ri} k_{ri} (l_{ri} / \delta_{ri})^{a_{ri}}}_{\text{Fuel cost}} \\
 & - \underbrace{C^{Hold} \sum_{(r,i,s,j) \in Q} \sum_{\varepsilon \in \Omega} \pi_\varepsilon m_{risj} \gamma_{risj}}_{\text{Holding cost of transshipment}} - \underbrace{\sum_{r \in R} \sum_{i \in I_r} C_{p_{ri}}^{Berth} \theta_{rib}}_{\text{Berth cost for extra usage}} - \underbrace{\sum_{p \in P} \sum_{w \in W} C_p^{Yard} \lambda_{pw}}_{\text{Yard cost for extra usage}}
 \end{aligned} \tag{1}$$

325

subject to

$$1 \leq \beta_r \leq N_r^{Ship} \quad r \in R \tag{2}$$

$$0 \leq \tau_{r1} \leq 6 \quad r \in R \tag{3}$$

$$\delta_{ri} \geq T_{ri}^{Leg} \quad r \in R, i \in I_r \tag{4}$$

$$\tau_{r,i+1} = \tau_{ri} + d_{ri} + \delta_{ri} \quad r \in R, i \in I_r \tag{5}$$

$$\tau_{r,|I_r|+1} = \tau_{r1} + 7\beta_r \quad r \in R \tag{6}$$

$$\sum_{w \in W} \eta_{riw} = 1 \quad r \in R, i \in I_r \tag{7}$$

$$\tau_{ri} = \sum_{w \in W} w \eta_{riw} + 7\zeta_{ri} \quad r \in R, i \in I_r \tag{8}$$

$$0 \leq \zeta_{ri} \leq \beta_r - 1 \quad r \in R, i \in I_r \tag{9}$$

$$\tau_{sj} - \tau_{ri} + 7\xi_{risj} = \gamma_{risj} \quad (r, i, s, j) \in Q \tag{10}$$

$$0 \leq \gamma_{risj} \leq 6 \quad (r, i, s, j) \in Q \tag{11}$$

$$\sum_{b \in B_{p_{ri}} \cup \{\hat{b}\}} \theta_{rib} = 1 \quad r \in R, i \in I_r \tag{12}$$

$$\sum_{r \in R'_p} \sum_{v=1}^{\bar{D}} \sum_{i \in I'_{rp}: d_{ri}=v} \sum_{k=0}^{v-1} \theta_{rib} \eta_{r,i,(w-k+7) \bmod 7} \leq g_{bw} \quad p \in P, b \in B_p, w \in W \tag{13}$$

$$\left(\sum_{(r,i,s,j) \in Q_p} \sum_{\varepsilon \in \Omega} \pi_\varepsilon m_{risj\varepsilon} \sum_{\dot{w}, \ddot{w} \in W} \eta_{ri\dot{w}} \eta_{sj\ddot{w}} f_{\dot{w}\ddot{w}} - A_p^{Port} \right)^+ = \lambda_{pw} \quad p \in P, w \in W \quad (14)$$

$$\sum_{\varepsilon \in \Omega} \pi_\varepsilon n_{ri\varepsilon} \leq A_{ri}^{Vol} \quad r \in R, i \in I_r \quad (15)$$

$$Prob\left(\sum_{\varepsilon \in \Omega} \sum_{u=1}^{\lceil \pi_\varepsilon n_{ri\varepsilon} \rceil} \tilde{c}_{ri\varepsilon u} > A_{ri}^{Load}\right) \leq \alpha \quad r \in R, i \in I_r \quad (16)$$

$$0 \leq \pi_\varepsilon \leq 1 \quad \varepsilon \in \Omega \quad (17)$$

$$\beta_r \in \mathbb{Z}_+ \quad r \in R \quad (18)$$

$$\tau_{ri} \in \mathbb{Z}_+ \cup \{0\} \quad r \in R, i \in I_r \cup \{|I_r| + 1\} \quad (19)$$

$$\eta_{riw} \in \{0, 1\} \quad r \in R, i \in I_r, w \in W \quad (20)$$

$$\delta_{ri} \in \mathbb{Z}_+ \cup \{0\} \quad r \in R, i \in I_r \quad (21)$$

$$\zeta_{ri} \in \mathbb{Z}_+ \cup \{0\} \quad r \in R, i \in I_r \quad (22)$$

$$\gamma_{risj} \in \mathbb{Z}_+ \cup \{0\} \quad (r, i, s, j) \in Q \quad (23)$$

$$\xi_{risj} \in \mathbb{Z} \quad (r, i, s, j) \in Q \quad (24)$$

$$\theta_{rib} \in \{0, 1\} \quad r \in R, i \in I_r, b \in B_{p_{ri}} \cup \{\hat{b}\} \quad (25)$$

$$\lambda_{pw} \geq 0 \quad p \in P, w \in W. \quad (26)$$

326 The objective (1) is to maximize the revenue, minus the five types of cost
327 described in Section 3. Constraints (2) state that at least one ship and at most N_r^{Ship}
328 ships should be deployed on each route. Constraints (3) ensure the start time of each
329 route (service) occurs in the first week. Constraints (4) relate to the minimum re-
330 quired sailing time T_{ri}^{Leg} for each leg, which depends on the maximum speed of ships.
331 Constraints (5) link the arrival time τ_{ri} of a port of call with the arrival time $\tau_{r,i+1}$
332 of the next port of call on a route. Constraints (6) guarantee that the total number
333 of days $\tau_{r,|I_r|+1} - \tau_{r1}$ for a ship completing its travel on a route is the number of
334 ships deployed on the route times seven, because all the services follow weekly arrival
335 pattern and one week has seven days. Constraints (7)–(9) link the binary variable
336 η_{riw} and the integer variable τ_{ri} , both of which denote the arrival time of the i^{th}

337 port of call on ship route r . The difference is that τ_{ri} denotes the arrival time on a
 338 universal time axis, while μ_{ri}^w denotes the arrival time in one of the seven days in a
 339 week. The former is from the perspective of port arrival time in one ship's itinerary
 340 (e.g., day 2 at port 1, day 11 at port 2), while the latter is from the perspective of
 341 the port arrival time of a fleet of ships deployed on a route (e.g., Mon at port 1,
 342 Wed at port 2). Constraints (10)–(11) transfer the absolute time gap (days) $\tau_{sj} - \tau_{ri}$
 343 between two ports of call (r, i) and (s, j) to a time difference γ_{risj} in days within one
 344 week. Similarly, the former is from the perspective of port arrival time in two ship's
 345 itineraries for two routes (e.g., a ship in route 1 arrives at port p on day 2, a ship
 346 in route 2 arrives at the port p on day 11, and the absolute time difference is nine
 347 days), while the latter is from the perspective of the port arrival time of two fleets of
 348 ships deployed on two routes (e.g., route 1's fleet arrives at the port on Mon, route
 349 2's fleet arrives at the port on Wed, and the time difference is two days, which is the
 350 waiting time for transshipment from route 1 to route 2). Constraints (12) guarantee
 351 that each port of call of a route should be assigned a berth (one of reserved berths or
 352 the dummy berth \hat{b}). The berth availability limitation is ensured by Constraints (13),
 353 which are not straightforward and will be explained later. Constraints (14) calculate
 354 the extra used yard space (TEUs) for storing transshipped containers at each port on
 355 each day. Constraints (15) define the limitation of the ship capacity with respect to
 356 its available space during each leg. Constraints (16) mean that the overload probabili-
 357 ty is lower than a threshold α . Constraints (17)–(26) state the ranges of the defined
 358 decision variables.

359 More explanations are required for Constraints (13). In the simplest case where
 360 all ships dwell at ports for only one day, the left-hand side of the constraint is
 361 $\sum_{r \in R'_p} \sum_{i \in I'_{rp}} \theta_{rib} \eta_{riw}$, which denotes whether or not one of the reserved berths b
 362 is used by a ship on day w in a week. This value should not be greater than g_{bw} ,
 363 which is the availability of the berth. If some ships dwell at a port for one day (i.e.,
 364 $d_{ri} = 1$), and some ships dwell for two days (i.e., $d_{ri} = 2$), the calculation on whether
 365 or not berth b is used by the i^{th} port of call on ship route r is as follows: (1) if w
 366 $= 1, 2, 3, \dots, 6$, then $\sum_{r \in R'_p} [\sum_{i \in I'_{rp}: d_{ri}=1} \theta_{rib} \eta_{riw} + \sum_{i \in I'_{rp}: d_{ri}=2} (\theta_{rib} \eta_{r,i,w-1} + \theta_{rib} \eta_{riw})]$;
 367 (2) if $w = 0$, then $\sum_{r \in R'_p} [\sum_{i \in I'_{rp}: d_{ri}=1} \theta_{rib} \eta_{riw} + \sum_{i \in I'_{rp}: d_{ri}=2} (\theta_{rib} \eta_{r,i,w-1+7} + \theta_{rib} \eta_{riw})]$.
 368 In what follows, subscripts $w - 1$ and $w - 1 + 7$ are interpreted as $(w - 1 + 7) \bmod$
 369 7. Then suppose the ships' dwell time can be one, two, \dots , or at most \bar{D} days, then

370 the above formula becomes $\sum_{r \in R'_p} \sum_{v=1}^{\bar{D}} \sum_{i \in I'_{rp}: d_{ri}=v} \sum_{k=0}^{v-1} (\theta_{rib} \eta_{r,i,(w-k+7) \bmod 7})$. This
 371 value does not exceed g_{bw} by Constraints (13).

372 5. Linearization of the model

373 The above model **[M1]** is an optimization problem with integer decision variables
 374 and non-linear terms that are non-convex. It is difficult to solve it using off-the-shelf
 375 solvers because (i) it contains a large number of discrete variables and (ii) it has a
 376 non-linear objective function and non-linear constraints. To solve this model, we first
 377 linearize it, and we then develop a sequential optimization algorithm.

378 5.1. Linearization of Objective (1)

379 Objective (1) contains a non-linear part $\sum_{r \in R} \sum_{i \in I_r} l_{ri} k_{ri} (l_{ri} / \delta_{ri})^{a_{ri}}$, which can
 380 be rewritten as $\sum_{r \in R} \sum_{i \in I_r} l_{ri} k_{ri} l_{ri}^{a_{ri}} \delta_{ri}^{-a_{ri}}$. The key is to transform $\delta_{ri}^{-a_{ri}}$ into a linear
 381 form. We adopt the linearization method used by Wang et al. (2013). We first redefine
 382 δ_{ri} as a new binary variable δ'_{rit} , which denotes whether or not the sailing time for
 383 the i^{th} leg of ship route r equals t days, $t \in T$, where T is the set of integers denoting
 384 the possible sailing times (in days) for all legs; for example $T \in \{1, \dots, 15\}$. The
 385 non-linear form $\delta_{ri}^{-a_{ri}}$ can then be replaced with $\sum_{t \in T} \delta'_{rit} t^{-a_{ri}}$, subject to $\sum_{t \in T} \delta'_{rit} = 1$
 386 for all $r \in R, i \in I_r$.

387 Objective (1) contains another non-linear part $\sum_{(r,i,s,j) \in Q} \pi_\varepsilon m_{risj\varepsilon} \gamma_{risj}$, which can
 388 be linearized as follows Alharbi et al. (2015). We first transform the integer variable
 389 γ_{risj} into a binary variable. Since $\gamma_{risj} \in W$, we redefine γ_{risj} as a binary variable
 390 γ'_{risjw} , equal to one if and only if the time gap between ports of call (r, i) and (s, j)
 391 is w days. Then γ_{risj} is replaced with $\sum_{w \in W} w \gamma'_{risjw}$, subject to $\sum_{w \in W} \gamma'_{risjw} = 1$ for
 392 all $(r, i, s, j) \in Q$. Here both π_ε and γ'_{risjw} are binary variables; therefore, the value
 393 of M is 1.

394

Based on the above linearization, Objective (1) becomes

$$\begin{aligned}
\text{Maximize } Z = & \underbrace{\sum_{\varepsilon \in \Omega} V_\varepsilon \pi_\varepsilon}_{\text{Revenue}} - \underbrace{\sum_{r \in R} C_r^{Opr} \beta_r}_{\text{Ship operation cost}} - \underbrace{\sum_{r \in R} \sum_{i \in I_r} l_{ri} k_{ri} l_{ri}^{a_{ri}} \sum_{t \in T} \delta'_{rit} t^{-a_{ri}}}_{\text{Fuel cost}} \\
& - \underbrace{C^{Hold} \sum_{(r,i,s,j) \in Q} \sum_{w \in W} m_{risj\varepsilon} w Q_{risjw\varepsilon}}_{\text{Holding cost of transshipment}} - \underbrace{\sum_{r \in R} \sum_{i \in I_r} C_{pri}^{Berth} \theta_{rib}}_{\text{Berth cost for extra usage}} - \underbrace{\sum_{p \in P, w \in W} C_p^{Yard} \lambda_{pw}}_{\text{Yard cost for extra usage}}
\end{aligned} \tag{27}$$

395

396

The newly defined variables and constraints needed for this linearization are summarized as follows:

397

Newly defined indices, sets and parameters:

398

t index of the number of days;

399

T set of possible numbers of days for a leg's sailing time, $T = \{1, \dots, |T|\}$;

400

M a sufficiently large positive number.

401

Newly defined variables:

402

δ'_{rit} a binary variable equal to one if and only if the sailing time of the leg (r, i) is t ;

403

γ'_{risjw} a binary variable equal to one if and only if the time gap between the ports of call (r, i) and (s, j) (i.e., γ_{risj}) is w days;

404

$Q_{risjw\varepsilon}$ continuous variable equal to $\pi_\varepsilon \gamma'_{risjw}$ if $\gamma'_{risjw} = 1$; otherwise zero.

405

Newly defined constraints:

Constraints (11) are removed. Constraints (5), (10), (21), (23) are replaced with the following four constraints, respectively.

$$\tau_{r,i+1} = \tau_{ri} + d_{ri} + \sum_{t \in T} t \delta'_{rit} \quad r \in R, i \in I_r \tag{28}$$

$$\tau_{sj} - \tau_{ri} + 7\xi_{risj} = \sum_{w \in W} w \gamma'_{risjw} \quad (r, i, s, j) \in Q \tag{29}$$

$$\delta'_{rit} \in \{0, 1\} \quad r \in R, i \in I_r, t \in T \tag{30}$$

$$\gamma'_{risjw} \in \{0, 1\} \quad (r, i, s, j) \in Q, w \in W. \quad (31)$$

In addition, four new constraints are defined:

$$\sum_{t \in T} \delta'_{rit} = 1 \quad r \in R, i \in I_r \quad (32)$$

$$\sum_{w \in W} \gamma'_{risjw} = 1 \quad (r, i, s, j) \in Q \quad (33)$$

$$0 \leq \varrho_{risjw\varepsilon} \leq 1 \quad (r, i, s, j) \in Q, w \in W, \varepsilon \in \Omega. \quad (34)$$

406 5.2. Linearization of Constraints (13)

407 Constraints (13) contain a non-linear part $\theta_{rib}\eta_{r,i,(w-k+7) \bmod 7}$, which is the prod-
408 uct of two binary variables. Following the method used by Yi et al. (2018), we define
409 a new binary variable φ_{ribw} to replace the non-linear part.

410 **Newly defined variables:**

411 φ_{ribw} binary variable equal to one if and only if the ship arrives at the berth b
on the day w of a week in the i^{th} port of call on ship route r .

Then Constraints (13) become

$$\sum_{r \in R'_p} \sum_{v=1}^{\bar{D}} \sum_{i \in I'_r: d_{ri}=v} \sum_{k=0}^{v-1} \theta_{r,i,b,(w-k+7) \bmod 7} \leq g_{bw} \quad p \in P, b \in B_p, w \in W. \quad (35)$$

In addition, some more constraints need to be defined so that the newly defined
variable φ_{ribw} can replace the function of $\theta_{rib}\eta_{r,i,(w-k+7) \bmod 7}$.

$$\varphi_{ribw} \geq \theta_{rib} + \eta_{riw} - 1 \quad r \in R, i \in I_r, b \in B_{p_{ri}}, w \in W \quad (36)$$

$$\varphi_{ribw} \leq \theta_{rib} \quad r \in R, i \in I_r, b \in B_{p_{ri}}, w \in W \quad (37)$$

$$\varphi_{ribw} \leq \eta_{riw} \quad r \in R, i \in I_r, b \in B_{p_{ri}}, w \in W \quad (38)$$

$$\varphi_{ribw} \in \{0, 1\} \quad r \in R, i \in I_r, b \in B_{p_{ri}}, w \in W. \quad (39)$$

412 5.3. Linearization of Constraints (14)

413 Constraints (14) contain the product of three variables $\pi_\varepsilon, \eta_{riw}$ and $\eta_{sj\bar{w}}$. In ad-
414 dition, the form $\lambda_{pw} = (\cdot)^+$ is also non-linear. In the first case, we use an approach

415 similar to that of Section 5.2 to handle it. This approach was used by Wang and
 416 Meng (2012). We define some more decision variables and constraints:

417 **Newly defined variables:**

418 $\psi_{risj\dot{w}\ddot{w}}$ binary variable equal to one if and only if both variables $\eta_{ri\dot{w}}$ and $\eta_{sj\ddot{w}}$
 are equal to one;

$\phi_{risj\dot{w}\ddot{w}\varepsilon}$ binary variable equal to π_ε if and only if $\psi_{risj\dot{w}\ddot{w}} = 1$.

Then Constraints (14) become

$$\lambda_{pw} = \left(\sum_{(r,i,s,j) \in Q_p} \sum_{\varepsilon \in \Omega} \sum_{\dot{w}, \ddot{w} \in W} m_{risj\varepsilon} f_{\dot{w}\ddot{w}} \phi_{risj\dot{w}\ddot{w}\varepsilon} - A_p^{Port} \right)^+ \quad p \in P, w \in W. \quad (40)$$

In addition, some more constraints need to be defined as follows so that the newly defined variable $\psi_{risj\dot{w}\ddot{w}}$ can replace the function of $\eta_{ri\dot{w}}\eta_{sj\ddot{w}}$:

$$\psi_{risj\dot{w}\ddot{w}} \geq \eta_{ri\dot{w}} + \eta_{sj\ddot{w}} - 1 \quad (r, i, s, j) \in Q; \dot{w}, \ddot{w} \in W \quad (41)$$

$$\psi_{risj\dot{w}\ddot{w}} \leq \eta_{ri\dot{w}} \quad (r, i, s, j) \in Q; \dot{w}, \ddot{w} \in W \quad (42)$$

$$\psi_{risj\dot{w}\ddot{w}} \leq \eta_{sj\ddot{w}} \quad (r, i, s, j) \in Q; \dot{w}, \ddot{w} \in W \quad (43)$$

$$\psi_{risj\dot{w}\ddot{w}} \in \{0, 1\} \quad (r, i, s, j) \in Q; \dot{w}, \ddot{w} \in W \quad (44)$$

$$\phi_{risj\dot{w}\ddot{w}\varepsilon} \geq \pi_\varepsilon + (\psi_{risj\dot{w}\ddot{w}} - 1)M \quad (r, i, s, j) \in Q; \dot{w}, \ddot{w} \in W, \varepsilon \in \Omega \quad (45)$$

$$0 \leq \phi_{risj\dot{w}\ddot{w}\varepsilon} \leq 1 \quad (r, i, s, j) \in Q; \dot{w}, \ddot{w} \in W, \varepsilon \in \Omega. \quad (46)$$

For the non-linear part $\lambda_{pw} = (\cdot)^+$, we adopt the linearization method used by Wang and Meng (2015). We define two more non-negative variables λ_{pw}^+ and λ_{pw}^- , and Constraints (40) are changed into

$$\sum_{(r,i,s,j) \in Q_p} \sum_{\varepsilon \in \Omega} \sum_{\dot{w}, \ddot{w} \in W} m_{risj\varepsilon} f_{\dot{w}\ddot{w}} \phi_{risj\dot{w}\ddot{w}\varepsilon} - A_p^{Port} = \lambda_{pw}^+ - \lambda_{pw}^- \quad p \in P, w \in W. \quad (47)$$

Then Constraints (26) are replaced with

$$\lambda_{pw}^+, \lambda_{pw}^- \geq 0 \quad p \in P, w \in W. \quad (48)$$

419 Moreover, Objective (27) is further restated by replacing λ_{pw} with λ_{pw}^+ . Then
 420 the final version of the objective becomes

$$\begin{aligned}
 \text{Maximize } Z = & \underbrace{\sum_{\varepsilon \in \Omega} V_\varepsilon \pi_\varepsilon}_{\text{Revenue}} - \underbrace{\sum_{r \in R} C_r^{Opr} \beta_r}_{\text{Ship operation cost}} - \underbrace{\sum_{r \in R} \sum_{i \in I_r} l_{ri} k_{ri} l_{ri}^{a_{ri}} \sum_{t \in T} \delta'_{rit} t^{-a_{ri}}}_{\text{Fuel cost}} \\
 & - \underbrace{C^{Hold} \sum_{\langle r, i, s, j \rangle \in Q} \sum_{w \in W} m_{risj\varepsilon} w Q_{risjw\varepsilon}}_{\text{Holding cost of transshipment}} - \underbrace{\sum_{r \in R} \sum_{i \in I_r} C_{pri}^{Berth} \theta_{rib}}_{\text{Berth cost for extra usage}} - \underbrace{\sum_{p \in P, w \in W} C_p^{Yard} \lambda_{pw}^+}_{\text{Yard cost for extra usage}}.
 \end{aligned} \tag{49}$$

421 **Lemma 1.** *Because the weights of the $[\pi_\varepsilon n_{ri\varepsilon}]$ containers are independent and i-*
 422 *dentically distributed random variables with expected values $u_{ri\varepsilon}$ and variances $\sigma_{ri\varepsilon}^2$,*
 423 *the classical central limit theorem (CLT) states that since $[\pi_\varepsilon n_{ri\varepsilon}]$ is very large,*
 424 *the distribution of the total weight $\sum_{u=1}^{[\pi_\varepsilon n_{ri\varepsilon}]} \tilde{c}_{ri\varepsilon u}$ is approximately normal with mean*
 425 *$[\pi_\varepsilon n_{ri\varepsilon}] \mu_{ri\varepsilon}$ and variance $[\pi_\varepsilon n_{ri\varepsilon}] \sigma_{ri\varepsilon}^2$.*

426 **Lemma 2.** *When $[\pi_\varepsilon n_{ri\varepsilon}]$ is very large, $r \in R, i \in I_r, \varepsilon \in \Omega$, since the containers*
 427 *weights are independent, the total weight $\sum_{\varepsilon \in \Omega} \sum_{u=1}^{[\pi_\varepsilon n_{ri\varepsilon}]} \tilde{c}_{ri\varepsilon u}$ of all the carried con-*
 428 *tainers approximately follows a normal distribution $N(\sum_{\varepsilon \in \Omega} [\pi_\varepsilon n_{ri\varepsilon}] \mu_{ri\varepsilon},$*
 429 *$\sum_{\varepsilon \in \Omega} [\pi_\varepsilon n_{ri\varepsilon}] \sigma_{ri\varepsilon}^2$).*

In reality, the number of containers is large. According to Lemma (2), Constraints (16) can be approximated by

$$\sum_{\varepsilon \in \Omega} [\pi_\varepsilon n_{ri\varepsilon}] \mu_{ri\varepsilon} + z_{1-\alpha} \left(\sum_{\varepsilon \in \Omega} [\pi_\varepsilon n_{ri\varepsilon}] \sigma_{ri\varepsilon}^2 \right)^{\frac{1}{2}} \leq A_{ri}^{Load} \quad r \in R, i \in I_r, \tag{50}$$

430 where $z_{1-\alpha}$ is the 100(1 - α) percentile of the standard normal distribution.

431 **Proposition 1.** *The left-hand sides of Constraints (50) are in general non-convex*
 432 *in π_ε .*

433 *Proof.* To prove the proposition, we just need to provide a non-convex example.
 434 Consider a simple case with only one OD pair, i.e., $|\Omega| = 1$. Suppose that for this
 435 OD pair ε , we have $\mu = 1, \sigma^2 = 0.25$. Suppose further than $z = 1$ and $n_{ri\varepsilon} = 10$. Then
 436 the left-hand side of the constraint becomes $10\pi + 0.25\sqrt{10\pi}$. Consider three values of

437 π : $\pi_1 = 0$, $\pi_2 = 1$, and $\pi_3 = 2$. Then $10\pi_1 + 0.25\sqrt{10\pi_1} = 0$, $10\pi_2 + 0.25\sqrt{10\pi_2} = 1.25$,
438 $10\pi_3 + 0.25\sqrt{10\pi_3} = 2.35$. In other words, $\pi_2 = (\pi_1 + \pi_3)/2 = (0 + 2)/2 = 1$, however,
439 $10\pi_2 + 0.25\sqrt{10\pi_2} > (10\pi_1 + 0.25\sqrt{10\pi_1} + 10\pi_3 + 0.25\sqrt{10\pi_3})/2$. Therefore, the left-
440 hand side of the constraint in this case is non-convex. \square

441 In order to handle the non-convex Constraints (50), we propose a second-order
442 cone programming (SOCP)-based algorithm, which will be elaborated in Section 6.

443 6. Algorithmic strategy

444 We now present an SOCP-based algorithm to handle non-convex constraints in the
445 model. A dynamic linearization algorithm and a tabu search algorithm are applied
446 to solve the model under different scales of route networks.

447 6.1. SOCP transformation

We use SOCP to transfer Constraints (50) to a convex one. We first define a new
binary variable $\kappa_{ri\varepsilon h}$ to represent the integer $\lceil \pi_\varepsilon n_{ri\varepsilon} \rceil$:

$$\lceil \pi_\varepsilon n_{ri\varepsilon} \rceil = \sum_{h=0}^{H_{ri\varepsilon}} 2^h \kappa_{ri\varepsilon h} \quad r \in R, i \in I_r, \varepsilon \in \Omega, h = 0, 1, \dots, H_{ri\varepsilon} \quad (51)$$

$$\sum_{h=0}^{H_{ri\varepsilon}} 2^h \kappa_{ri\varepsilon h} \leq n_{ri\varepsilon} \quad r \in R, i \in I_r, \varepsilon \in \Omega, h = 0, 1, \dots, H_{ri\varepsilon} \quad (52)$$

$$\kappa_{ri\varepsilon h} \in \{0, 1\} \quad r \in R, i \in I_r, \varepsilon \in \Omega, h = 0, 1, \dots, H_{ri\varepsilon}, \quad (53)$$

where $H_{ri\varepsilon} := \lfloor \log_2 n_{ri\varepsilon} \rfloor$. Then Constraints (50) become

$$\sum_{\varepsilon \in \Omega} \mu_{ri\varepsilon} \sum_{h=0}^{H_{ri\varepsilon}} 2^h \kappa_{ri\varepsilon h} + z_{1-\alpha} \left(\sum_{\varepsilon \in \Omega} \sigma_{ri\varepsilon}^2 \sum_{h=0}^{H_{ri\varepsilon}} 2^h \kappa_{ri\varepsilon h} \right)^{\frac{1}{2}} \leq A_{ri}^{Load} \quad r \in R, i \in I_r. \quad (54)$$

Since $\kappa_{ri\varepsilon h}$ is binary, we have $\kappa_{ri\varepsilon h} = \kappa_{ri\varepsilon h}^2$. Using this property, Constraints (54)
become

$$\left(\sum_{\varepsilon \in \Omega} \sum_{h=0}^{H_{ri\varepsilon}} 2^h \sigma_{ri\varepsilon}^2 \kappa_{ri\varepsilon h}^2 \right)^{\frac{1}{2}} \leq (A_{ri}^{Load} - \sum_{\varepsilon \in \Omega} \sum_{h=0}^{H_{ri\varepsilon}} 2^h \mu_{ri\varepsilon} \kappa_{ri\varepsilon h}) / z_{1-\alpha} \quad r \in R, i \in I_r. \quad (55)$$

448 Constraints (55) are convex and now the following [**M2**] is a mixed integer SOCP
 449 (MISOCP) model, which can be solved by off-the-shelf solvers such as CPLEX.

450 [**M2**] An MISOCP model: Objective (49)

451 subject to Constraints (2)–(4), (6)–(9), (11)–(12), (15)–(20), (22), (24)–(25), (28)–
 452 (39), (41)–(48), (52)–(53), (55).

453 6.2. Dynamic linearization for solving [**M2**]

454 We propose solving the MISOCP model [**M2**] by integer linear programming. The
 455 core idea is as follows: since Constraints (55) are convex, if we know an infeasible
 456 solution $\check{\mathbf{y}} := (\check{\kappa}_{ri\epsilon h}, r \in R, i \in I_r, \epsilon \in \Omega, h = 0, 1, 2, \dots, H_{ri\epsilon})$ that violates the non-
 457 linear Constraints (55), we can linearize the left-hand side $(\sum_{\epsilon \in \Omega} \sum_{h=0}^{H_{ri\epsilon}} 2^h \sigma_{ri\epsilon}^2 \kappa_{ri\epsilon h}^2)^{\frac{1}{2}}$
 458 of the constraint at $\check{\mathbf{y}}$. Note that $\frac{\partial (\sum_{\epsilon \in \Omega} \sum_{h=0}^{H_{ri\epsilon}} 2^h \sigma_{ri\epsilon}^2 \kappa_{ri\epsilon h}^2)^{\frac{1}{2}}}{\partial \kappa_{ri\epsilon h}} = \frac{2^h \sigma_{ri\epsilon}^2 \check{\kappa}_{ri\epsilon h}}{(\sum_{\epsilon \in \Omega} \sum_{h=0}^{H_{ri\epsilon}} 2^h \sigma_{ri\epsilon}^2 \check{\kappa}_{ri\epsilon h}^2)^{\frac{1}{2}}}$ at
 459 $\check{\mathbf{y}}$. Hence, we can add the resulting linear constraint to the model in order to cut off
 460 the infeasible solution $\check{\mathbf{y}}$, as well as some other infeasible solutions. We propose the
 following Algorithm 1 to solve model [**M2**] and we then prove its correctness.

Algorithm 1 Dynamic linearization algorithm for solving [**M2**]

Step 1. Define a set Ψ of generated intermediate infeasible solutions of $\mathbf{y} := (\kappa_{ri\epsilon h}, r \in R, i \in I_r, \epsilon \in \Omega, h = 0, 1, 2, \dots, H_{ri\epsilon})$. Initialize $\Psi \leftarrow \emptyset$.

Step 2. Solve model [**M3**] whose objective function is Eq. (49) subject to Constraints (2)–(4), (6)–(9), (11)–(12), (15)–(20), (22), (24)–(25), (28)–(39), (41)–(48), (52)–(53) and the following constraints:

$$\frac{\sum_{\epsilon \in \Omega} \sum_{h=0}^{H_{ri\epsilon}} 2^h \sigma_{ri\epsilon}^2 \check{\kappa}_{ri\epsilon h} (\kappa_{ri\epsilon h} - \check{\kappa}_{ri\epsilon h})}{(\sum_{\epsilon \in \Omega} \sum_{h=0}^{H_{ri\epsilon}} 2^h \sigma_{ri\epsilon}^2 \check{\kappa}_{ri\epsilon h}^2)^{\frac{1}{2}}} + \left(\sum_{\epsilon \in \Omega} \sum_{h=0}^{H_{ri\epsilon}} 2^h \sigma_{ri\epsilon}^2 \check{\kappa}_{ri\epsilon h}^2 \right)^{\frac{1}{2}} \leq \quad (56)$$

$$\frac{A_{ri}^{Load} - \sum_{\epsilon \in \Omega} \sum_{h=0}^{H_{ri\epsilon}} 2^h \mu_{ri\epsilon} \kappa_{ri\epsilon h}}{z_{1-\alpha}}, \check{\mathbf{y}} \in \Psi, r \in R, i \in I_r.$$

Let $\hat{\mathbf{y}}$ be the optimal solution to model [**M3**].

Step 3. Check whether $\hat{\mathbf{y}}$ satisfies Constraints (55). If yes, then $\hat{\mathbf{y}}$ is the optimal solution to [**M2**] and stop. Otherwise, set $\Psi \leftarrow \Psi \cup \{\hat{\mathbf{y}}\}$ and go to **Step 1**.

462 **Proposition 2.** *No solution will be generated twice in Algorithm 1.*

463 *Proof.* If a generated solution $\hat{\mathbf{y}}$ is feasible with respect to Constraints (55), then the
 464 algorithm stops and hence it will not be generated twice. If it is infeasible, then it
 465 will become an element of Ψ at the next iteration and we denote it by $\check{\mathbf{y}}$. Since $\check{\mathbf{y}}$ is
 466 infeasible, we have

$$\left(\sum_{\varepsilon \in \Omega} \sum_{h=0}^{H_{ri\varepsilon}} 2^h \sigma_{ri\varepsilon}^2 \check{\kappa}_{ri\varepsilon h}^2 \right)^{\frac{1}{2}} > \frac{A_{ri}^{Load} - \sum_{\varepsilon \in \Omega} \sum_{h=0}^{H_{ri\varepsilon}} 2^h \mu_{ri\varepsilon} \check{\kappa}_{ri\varepsilon h}}{z_{1-\alpha}} \quad r \in R, i \in I_r. \quad (57)$$

467 Inequality (57) implies that $\hat{\mathbf{y}} = \check{\mathbf{y}}$ violates the added Constraints (56). Hence, $\hat{\mathbf{y}} = \check{\mathbf{y}}$
 468 will not be generated again. \square

469 **Proposition 3.** *Algorithm 1 terminates in a finite number of iterations.*

470 *Proof.* Since all $\kappa_{ri\varepsilon h}$ variables are binary for $r \in R, i \in I_r, \varepsilon \in \Omega$, and $h = 0, 1, \dots$
 471 $\cdot, H_{ri\varepsilon}$, the number of solutions feasible to Constraints (2)–(4), (6)–(9), (11)–(12),
 472 (15)–(20), (22), (24)–(25), (28)–(39), (41)–(48) and (52)–(53) is at most $2^{\sum_{r \in R} \sum_{i \in I_r} \sum_{\varepsilon \in \Omega} (1+H_{ri\varepsilon})}$.
 473 Proposition 2 implies that at least one solution is excluded at each iteration. Hence,
 474 Algorithm 1 terminates in at most $2^{\sum_{r \in R} \sum_{i \in I_r} \sum_{\varepsilon \in \Omega} (1+H_{ri\varepsilon})}$ iterations. \square

475 **Proposition 4.** *An optimal solution is obtained when Algorithm 1 terminates.*

476 *Proof.* Model $[\mathbf{M3}]$ is a relaxation of the original model $[\mathbf{M2}]$, because the lin-
 477 earization on the left-hand side of inequality (56) underestimates the convex function
 478 $\left(\sum_{\varepsilon \in \Omega} \sum_{h=0}^{H_{ri\varepsilon}} 2^h \sigma_{ri\varepsilon}^2 \kappa_{ri\varepsilon h}^2 \right)^{\frac{1}{2}}$. Since $[\mathbf{M2}]$ and $[\mathbf{M3}]$ have the same objective function, the
 479 value of $\hat{\mathbf{y}}$ generated in **Step 1** is at least equal to that of the optimal value of $[\mathbf{M2}]$.
 480 If $\hat{\mathbf{y}}$ is feasible for $[\mathbf{M2}]$, then the objective value of the feasible solution $\hat{\mathbf{y}}$ to $[\mathbf{M2}]$
 481 is equal to an upper bound (the optimal objective value of $[\mathbf{M3}]$), meaning that $\hat{\mathbf{y}}$
 482 is optimal for $[\mathbf{M2}]$. \square

483 6.3. Tabu search algorithm for solving $[\mathbf{M2}]$

484 We now propose a tabu search algorithm to solve $[\mathbf{M2}]$. Tabu search algorithm,
 485 introduced by Glover (1986), is an adaptive local iterative search that operates within

486 a solution space. It moves from one solution to another and diversifies solutions
 487 so as to find a better one (Vivaldini et al., 2016). At each iteration, the search
 488 process is applied to explore the neighborhood of the current optimal solution. Tabu
 489 search algorithm has often been applied to problems solving in the maritime industry.
 490 Cordeau et al. (2005) applied a tabu search algorithm to the berth allocation problem
 491 (BAP). Tirado et al. (2013) solved a dynamic and stochastic cargo transportation
 492 problem by means of tabu search. Nikolopoulou et al. (2017) used tabu search to
 493 compare two kinds of cargo transportation methods in the shipping industry.

494 *6.3.1. Local optimization using tabu search*

495 Given a neighborhood structure ($N(p_c)$) and an initial solution p , the tabu search
 496 algorithm iteratively replaces the incumbent solution p_c by a best eligible neighbor
 497 solution ($\hat{p} \in N(p_c)$) until a stopping criterion is met, i.e., the current optimal solution
 498 p^* has not been improved for T_{max} consecutive iterations. At each iteration, the best
 499 movement is recorded in the tabu list to prevent the reverse movement in the next
 500 iterations. A movement is eligible if it is not in the tabu list or if it results in a better
 501 solution than the current optimal solution. The general tabu search framework is
 502 described in Algorithm 2 and the details are explained in subsequent sections.

503 *6.3.2. Population initialization*

504 The population initialization is obtained by generating 10 random solutions using
 505 a uniform probability distribution. The component $x_{r,i}$ of each solution is randomly
 506 assigned a value from $[T_{ri}^{min}, T_{ri}^{max}]$, where $r \in R, i \in I_r \setminus \{|I_r|\}$. The minimum value
 507 T_{ri}^{min} and maximum value T_{ri}^{max} refer to the minimum sailing time and the maximum
 508 sailing time of each leg of each route according to the maximum speed and minimum
 509 sailing speed, respectively. Moreover, we should guarantee that the sum of the sailing
 510 time on each leg plus the duration time at each port is the multiple of seven by
 511 adjusting the time of the last component $x_{r,|I_r|}$, where $r \in R$. We then select the best
 512 solution p_0 among the 10 random solutions as the initial solution p .

513 *6.3.3. Neighborhood structure and movement*

514 The neighborhood structure is the crucial component of the algorithm. The neigh-
 515 borhood $N(p_c)$ contains all solutions in which the value of one component is changed

516 to its immediate adjacent values. The neighborhood $N(p_c)$ is defined by the one-
517 change movement operator which consists of changing the current solution p_c of a
518 single component either from $x_{r,i}$ to $x_{r,i} + 1$ or from $x_{r,i}$ to $x_{r,i} - 1$, where $r \in R, i \in$
519 $I_r \setminus \{|I_r|\}$. Meanwhile, we should guarantee that the sum of the sailing time on each
520 leg plus the duration time on each port is the multiple of seven by adjusting the time
521 of the last component $x_{r,|I_r|}$, where $r \in R$. Given an incumbent solution p_c , the one-
522 change movement operator is composed of all possible solutions that can be obtained
523 by applying the one-change movement to p_c .

524 6.3.4. Sorted candidate solutions

525 The candidate solutions $(SCS_1, SCS_2, \dots, SCS_l, \dots, SCS_{C_{max}})$ are generated after
526 the movement is achieved, where C_{max} is the number of candidate solutions, and the
527 fitness values of the candidate solutions $(SCF_1, SCF_2, \dots, SCF_l, \dots, SCF_{C_{max}})$ are
528 sorted in non-increasing order by using the bubble sorting method. Bubble sorting is a
529 simple sort algorithm. It compares two adjacent elements SCF_l and SCF_{l+1} . If SCF_l
530 is less than SCF_{l+1} , which means their order is opposite, the two adjacent element
531 positions are exchanged and their corresponding candidate solution positions are also
532 updated. If SCF_l is greater than or equal to SCF_{l+1} , no transformation operation is
533 taken.

534 **Algorithm 2** Tabu search algorithm for the fleet deployment and demand
535 fulfillment for container shipping liners

536 **Input:** parameters $T_{ri}^{min}, T_{ri}^{max}, T_{max}, C_{max}, L_{max}, D_{max}, GBF$ // $P_{ri}^{min}, P_{ri}^{max}$ are the minimum
537 and maximum values of the initial solution with respect to r, i ; T_{max} is the given number of iterations
538 for t ; C_{max} is the number of candidate solutions; L_{max} is the tabu list size; D_{max} is the given number
539 of iterations for d ; GBF is the best fitness of all solutions

540 **Output:** the objective value

- 541 1: initialization: initial solution $p = p_0$ // p_0 is the best solution among the t random solutions
- 542 2: neighborhood structure $N(p)$
- 543 3: tabu list $L = \emptyset$
- 544 4: $GBF \leftarrow f(p)$
- 545 5: $f(p^*) \leftarrow GBF$ // p^* is the current optimal solution
- 546 6: $p_c \leftarrow p_0$ // p_c is the incumbent solution
- 547 7: $d \leftarrow 0$ // d counts the consecutive number of iterations in which p^* is not improved
- 548 8: $t \leftarrow 0$ // t counts the consecutive number of iterations where p^* is not updated
- 549 9: **while** $t < T_{max}$ **do**
- 550 10: find a best solution $\hat{p} \in \operatorname{argmax}_{N(p_c)} [f(p_c)]$ // \hat{p} keeps the best solution found

```

551 11: record the movement in the tabu list
552 12: if  $\hat{p} \notin L$  then
553 13:     move to the best neighbor  $p_c \leftarrow \hat{p}$ 
554 14:     update tabu list
555 15: else
556 16:     if  $f(\hat{p}) > f(p^*)$  then
557 17:         move to the best neighbor  $p_c \leftarrow \hat{p}$ 
558 18:          $GBF \leftarrow f(\hat{p}), f(p^*) \leftarrow GBF$ 
559 19:          $p^* \leftarrow \hat{p}, d \leftarrow 0, t \leftarrow 0$ 
560 20:         clean tabu list
561 21:     else if  $f(\hat{p}) \leq f(p^*)$  then
562 22:          $d \leftarrow d + 1$ 
563 23:          $t \leftarrow t + 1$ 
564 24:         if  $d = D_{max}$  then
565 25:             clean tabu list
566 26:              $sum \leftarrow 0$ 
567 27:             for  $r \in R$ 
568 28:                 for  $i \in I_r \setminus \{|I_r|\}$ 
569 29:                     generate a solution  $sol_{ri}$ , whose value is allocated from  $T_{ri}^{min}$  to  $T_{ri}^{max}$ 
570 30:                      $sum \leftarrow sum + sol_{ri}$ 
571 31:                 end for
572 32:                 adjust  $sol_{r,|I_r|}$  to guarantee  $sum$  is the multiple of seven days
573 33:             end for
574 34:             save the incumbent solution  $p_c \leftarrow (sol_{ri}, r \in R, i \in I_r)$ 
575 35:              $d \leftarrow 0$ 
576 36:         end if
577 37:     end if
578 38: end if
579 39: end while
580 40: return the objective value

```

581 6.3.5. Intensification and diversification strategies

582 The use of memory structures within a tabu search meta-heuristic has been proven
583 to create a flexible search behavior. A key element of the proposed framework is to
584 achieve a balance between search intensification and diversification. The intensifica-
585 tion strategy encourages move combinations and solution features that have appeared
586 to be effective during the search. In contrast, diversification is used to broaden the
587 exploration of the solution space. In our algorithm, the diversification strategy clean-
588 s the tabu list and then randomly generates a new solution. In lines 20 and 25-34
589 of Algorithm 2, we provide a description of our intensification and diversification

590 strategies.

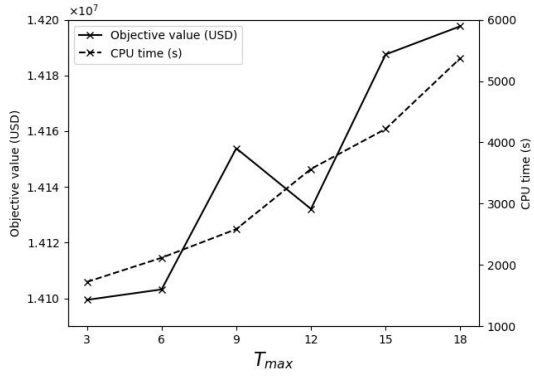
591 6.3.6. Sensitivity analysis of the parameters

592 To study the effectiveness of the proposed algorithm, we performed sensitivity
593 analyses to determine the optimal combination of heuristic parameters. The chosen
594 four parameters are the consecutive number of iterations where the current optimal
595 solution is not updated (T_{max}), the number of candidate solutions (C_{max}), the tabu
596 list size (L_{max}) and the consecutive number of iterations where the current optimal
597 solution is not improved (D_{max}). These parameters are key parameters which may
598 significantly affect the performance of the tabu search algorithm.

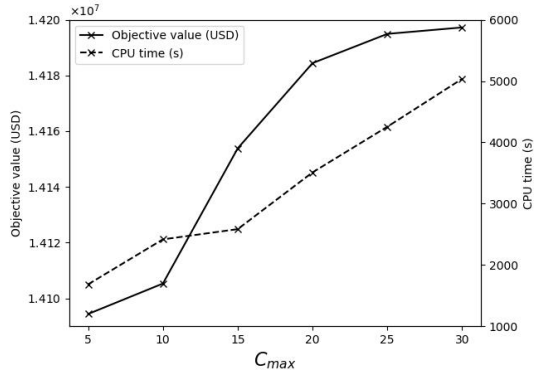
599 To show how the objective value and the computation time are influenced by
600 parameters T_{max} , C_{max} , L_{max} and D_{max} , we designed four test schemes. The outputs
601 consist of the computation time and the objective value. When we conduct sensi-
602 tivity analysis for one parameter, the values of the other three parameters are fixed.
603 Figure 2-(a) illustrates the interrelation between the value of parameter T_{max} and
604 the objective value as well as the computation time, with the value of T_{max} varying
605 in $\{3, 6, \dots, 18\}$. The same method is applied to parameters C_{max} , L_{max} and D_{max} ,
606 varying in $\{5, 10, \dots, 30\}$, $\{10, 20, \dots, 60\}$, and $\{3, 4, \dots, 8\}$, respectively.

607 The performance of tabu search algorithm is evaluated based on both the objective
608 value and the computation time. The results in Figure 2 show that with increases in
609 the values of parameters T_{max} , C_{max} , L_{max} and D_{max} , the computation times of the
610 tabu search algorithm rise considerably, which indicates that the computation times
611 are sensitive to the setting of parameters T_{max} , C_{max} , L_{max} and D_{max} . Interestingly,
612 the objective values of tabu search algorithm grow considerably with the values of
613 parameters T_{max} and C_{max} , but they fluctuate moderately as a function of L_{max} and
614 D_{max} , which illustrates that the objective values of tabu search algorithm are sensitive
615 to the setting of parameters T_{max} , C_{max} , but not to L_{max} and D_{max} .

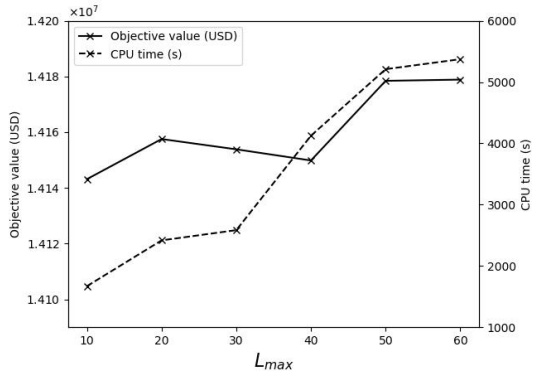
616 We then evaluated the performance of the tabu search algorithm over 36 instances
617 with fixed $L_{max} = 20$, $D_{max} = 4$ and different values of T_{max} and C_{max} . For each test
618 instance, several combinations of the two parameters T_{max} and C_{max} were used. The
619 objective values (left column) and the computational time (right column) of each test



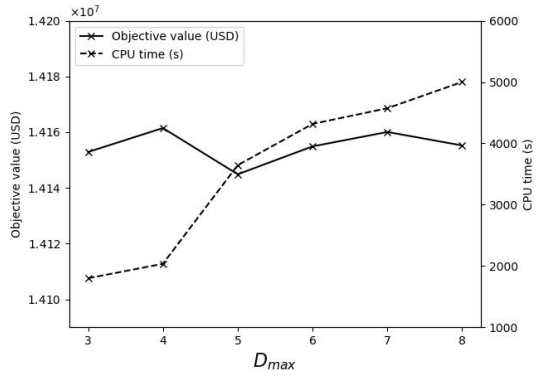
(a)



(b)



(c)



(d)

Figure 2: Sensitivity analysis of the parameters

Table 1: Influence of the parameters T_{max} and C_{max} on the performance of the tabu search heuristic

obj and time T_{max}	C_{max}		5	10	15	20	25	30				
4	14,102,397	1,568	14,150,993	1,733	14,159,445	2,518	14,160,098	3,022	14,178,442	3,426	14,192,053	3,677
6	14,140,967	1,821	14,137,802	2,200	14,104,409	2,212	14,135,676	3,454	14,170,465	3,672	14,200,567	4,348
8	14,130,444	1,577	14,143,956	2,417	14,143,855	2,584	14,192,930	3,510	14,137,544	4,255	14,179,581	5,037
10	14,184,778	2,055	14,167,990	2,343	14,210,744	2,555	14,193,398	4,022	14,202,056	4,709	14,188,033	5,633
12	14,150,376	3,734	14,180,336	3,723	14,192,098	3,554	14,197,544	4,392	14,179,002	4,430	14,207,834	5,722
14	14,192,804	4,271	14,192,003	3,356	14,199,581	4,598	14,190,095	4,765	14,201,566	5,221	14,198,892	5,576

Notes: (1) The objective values and the CPU time are recorded in the left column and right column, respectively. (2) The objective values and the CPU time are denoted by obj and time, respectively. (3) The CPU time is in seconds.

620 instance are recorded in Table 1. It can be seen that when $T_{max} \doteq 10$ and $C_{max} \doteq 15$,
621 we can obtain the best results. Therefore, the four values $T_{max}=10$, $C_{max} = 15$, L_{max}
622 $= 20$ and $D_{max} = 4$ will be used in the next experiments.

623 7. Computational experiments

624 In order to assess the effectiveness of the proposed decision model and the ef-
625 ficiency of our algorithms, we have carried out several computational experiments
626 on a LENOVO P910 workstation with 28 cores of CPUs, 2.4 GHz processing speed
627 and 256 GB of memory. All of the models and algorithms proposed in this article
628 were implemented in C# programming. The MIP models (the original model and the
629 submodels embedded in algorithms) were solved by CPLEX 12.5.1.

630 7.1. Instance setting

631 We first detail the setting of the model parameters. The value of V_ε relates to
632 the sailing distance and to the number of containers transported between an OD
633 pair. The sailing distance data can be obtained on the Internet websites, and the
634 unit container revenue data can be acquired on some logistics companies' official
635 websites. The average of C_r^{Opr} is set to 180,000 USD (Wang and Meng, 2015; Wang
636 et al., 2015; Alharbi et al., 2015). The average of N_r^{Ship} which depends on the length
637 of one cycle time is set to 20. This is consistent with the parameter setting used in
638 previous works (Wang and Xu, 2015; Yao et al., 2012). The average of k_{ri} is set to
639 0.25, and the average of a_{ri} is set to 2.6, which are basically the same as in previous
640 works (Wang et al., 2015; Bell et al., 2013; Yao et al., 2012; Wang and Meng, 2015;
641 Meng et al., 2016). The average of C^{Hold} is set to 20 USD per day per TEU (Zheng
642 et al., 2015; Wen et al., 2017; Wang and Meng, 2015; Bell et al., 2013). The value of
643 α is set to 1%. The maximum value of sailing speed is set to 22 knots, which is also
644 in line with the setting used in related works (Jiang and Jin, 2017; Wang et al., 2015;
645 Yao et al., 2012; Aydin et al., 2017). The average of C_p^{Berth} is set to 3000 per berth
646 (Chen et al., 2012) and the average of C_p^{Yard} is set to 200 USD per TEU (Jiang and
647 Jin, 2017). The value of \bar{D} is two days, which is consistent with realistic data from
648 the APL company.

649 The shipping network investigated in the numerical experiments is depicted in
650 Figure 1. The numbers of routes are three and four in the two different scales of

651 experiments, and the numbers of ports of call are four, four, five and six in route 1,
652 2, 3, and 4, respectively. The experimental instances are generated on the basis of a
653 specific rule. Taking the small-scale route network for example, the number of routes
654 is three and the numbers of ports of call are four, four, and five in route 1, 2, and 3,
655 respectively. We can then generate four cases in route 1, which differ from each other
656 only with respect to the ports of call. Each of the four cases uses three ports of call
657 among the four ports of call in the original route 1 shown in Figure 1. Analogously,
658 more sets of cases can be generated through different selections of ports of call in
659 other routes.

660 Thus for the small-scale without all ports of call network with three routes, there
661 are four sets of cases including three sets without all the ports of call, and an inte-
662 grated case with all of them. Similarly, as for the large-scale route network consisting
663 of four routes (as shown in Figure 1), there are four sets of cases without all ports of
664 call, and an integrated case with all of them.

665 *7.2. Investigating the efficiency of the proposed methods*

666 Here we apply the dynamic linearization algorithm to solve the model [M2].
667 A large number of numerical experiments on small-scale cases were carried out to
668 validate this algorithm by comparing the values of its solutions with the optimal
669 results obtained by CPLEX.

670 From the results shown in Table 2, the objective values obtained by the dynamic
671 linearization algorithm are equal to the optimal results, but this algorithm is faster
672 on the small-scale route network. Based on these observations, we can confirm the
673 efficiency of dynamic linearization algorithm. Table 2 also provides an upper bound
674 (UB) obtained by relaxing Constraints (15), and it shows the gap between the UB
675 and the optimal solution value, which is used to evaluate the efficiency of tabu search
676 algorithm in the large-scale route network. To generate a more complex shipping
677 network, we increase the number of routes from the three to four, which yields a
678 large-scale route network. The results of the experiments show that it is difficult to
679 obtain an optimal solution on this network within a reasonable time.

Table 2: Performance of the dynamic linearization (three routes)

Cases		CPLEX		Dynamic linearization				Upper Bound		
Num. of ports in three routes	ID	Z_C	T_C	π_ε	Z_D	T_D	GAP_C	$\frac{T_D}{T_C}$	Z_{UB}	GAP_{UB}
3-4-5 (Cases differ on the ports in route 1)	Case 1	2,550,670	43	90.34%	2,550,670	13	0.00%	0.30	2,557,281	0.26%
	Case 2	2,592,150	59	92.83%	2,592,150	11	0.00%	0.19	2,605,755	0.52%
	Case 3	2,450,207	28	91.90%	2,450,207	12	0.00%	0.43	2,463,843	0.56%
	Case 4	2,729,982	21	94.55%	2,729,982	8	0.00%	0.38	2,743,593	0.50%
4-3-5 (Cases differ on the ports in route 2)	Case 1	2,766,213	48	95.28%	2,766,213	12	0.00%	0.25	2,779,856	0.49%
	Case 2	2,959,825	73	94.46%	2,959,825	17	0.00%	0.23	2,969,885	0.34%
	Case 3	2,307,711	58	93.17%	2,307,711	10	0.00%	0.17	2,308,947	0.05%
	Case 4	2,648,636	27	93.35%	2,648,636	9	0.00%	0.33	2,652,364	0.14%
4-4-4 (Cases differ on the ports in route 3)	Case 1	2,354,829	30	91.96%	2,354,829	10	0.00%	0.33	2,368,568	0.58%
	Case 2	2,571,288	56	92.03%	2,571,288	12	0.00%	0.21	2,584,892	0.53%
	Case 3	2,667,825	28	93.30%	2,667,825	9	0.00%	0.32	2,671,536	0.14%
	Case 4	2,570,305	57	92.27%	2,570,305	12	0.00%	0.21	2,576,964	0.26%
	Case 5	2,664,537	35	94.82%	2,664,537	11	0.00%	0.31	2,668,272	0.14%
4-4-5	Case 1	3,905,795	75	93.11%	3,905,795	15	0.00%	0.20	3,921,398	0.40%
<i>Average</i>				93.10%			0.00%	0.28		0.35%

Notes: (1) The optimal objective values and the CPU time are denoted by Z_C and T_C , respectively. (2) The objective values and the CPU time of the dynamic linearization algorithm are denoted by Z_D and T_D , respectively. (3) $GAP_C = (Z_D - Z_C)/Z_C$, $GAP_{UB} = (Z_{UB} - Z_C)/Z_C$.

Table 3: Comparing dynamic linearization with tabu search (four routes)

Cases		Dynamic linearization			Tabu search		Comparison	
Num. of ports in four routes	ID	Z_D	$Time_D$	π_ϵ	Z_T	$Time_T$	GAP_{TD}	$\frac{Time_T}{Time_D}$
3-4-5-6 (Cases differ on the ports in route 1)	Case 1	11,038,551	3,180	92.02%	11,008,751	1,489	0.27%	0.47
	Case 2	11,874,243	2,692	91.44%	11,809,739	1,803	0.54%	0.67
	Case 3	11,728,095	3,034	93.56%	11,708,295	1,865	0.17%	0.61
	Case 4	12,133,870	1,872	94.47%	12,114,073	1,174	0.16%	0.63
4-3-5-6 (Cases differ on the ports in route 2)	Case 1	12,170,101	2,845	93.23%	12,124,114	1,687	0.38%	0.59
	Case 2	12,470,813	2,923	94.34%	12,421,430	2,075	0.40%	0.71
	Case 3	12,117,924	2,900	93.54%	12,098,124	2,126	0.16%	0.73
	Case 4	12,039,317	2,879	90.86%	11,999,518	2,020	0.33%	0.70
4-4-4-6 (Cases differ on the ports in route 3)	Case 1	11,893,770	3,045	92.88%	11,867,079	1,988	0.22%	0.65
	Case 2	12,178,122	3,300	94.32%	12,145,369	1,723	0.27%	0.52
	Case 3	12,058,507	2,954	95.63%	12,018,702	1,636	0.33%	0.55
	Case 4	11,051,646	2,326	92.32%	11,018,431	1,702	0.30%	0.73
	Case 5	12,069,020	3,875	93.64%	12,029,216	1,734	0.33%	0.45
4-4-5-5 (Cases differ on the ports in route 4)	Case 1	10,947,598	3,004	90.32%	10,927,708	1,556	0.18%	0.52
	Case 2	11,120,029	3,154	91.75%	11,080,223	2,164	0.36%	0.69
	Case 3	11,998,000	2,934	94.92%	11,958,243	2,171	0.33%	0.74
	Case 4	11,594,584	3,357	93.33%	11,554,784	1,947	0.34%	0.58
	Case 5	11,424,056	3,011	92.44%	11,363,650	1,436	0.53%	0.48
	Case 6	11,996,883	2,173	92.46%	11,957,174	1,309	0.33%	0.60
4-4-5-6	Case 1	14,284,795	4,503	90.02%	14,210,744	2,555	0.52%	0.57
<i>Average</i>				92.87%			0.32%	0.61

Notes: (1) $Time_D$ and $Time_T$ denote the CPU time of the dynamic linearization algorithm and tabu search algorithm, respectively. (2) $GAP_{TD} = (Z_D - Z_T)/Z_D$. (3) The CPU time is in seconds.

680 Therefore, we suggest applying tabu search algorithm to solve the model, and we
681 compare its objective value with that obtained by the dynamic linearization algorithm.
682 The results in the rightmost two columns of Table 3 demonstrate that the average
683 gap between dynamic linearization and tabu search algorithm is about 0.32%, but
684 the average ratio of the CPU time of tabu search algorithm to that of the dynamic
685 linearization algorithm is only 0.61, which indicates that tabu search may not on-
686 ly obtain near-optimal objective function values, but can also solve the model in a
687 much faster way. These results confirm the effectiveness of the dynamic linearization
688 algorithm and of the tabu search algorithm. They demonstrate that tabu search is
689 an effective method for solving the proposed model.

690 8. Conclusions

691 We have proposed an integrated optimization model for the fleet deployment and
692 demand fulfillment problem, with the consideration of overload risk of containers,
693 vessel size and port resources (e.g., berths, yard space). The objective was to jointly
694 optimize the number of ships in each route, the ship speed on each leg, the visiting
695 time of ships at each port of call, and the fulfillment scale of each OD pair's demand.
696 Since the proposed model is a chance-constrained non-linear MIP model, we have
697 suggested some novel techniques to linearize it into a tractable MISOCP model for
698 some commercial solvers such as the CPLEX. Two efficient algorithms were then
699 suggested to solve the model under different scales of route networks. The proposed
700 model as well as the algorithms can help shipping liners plan the deployment and
701 scheduling of ships along each route. Numerical experiments based on real-world data
702 were conducted to validate the effectiveness of our decision model and the efficiency
703 of the proposed solution methods. With respect to the large body of research on liner
704 ship fleet deployment, we have made three main new contributions:

705 (1) Few of the previous fleet deployment related studies have considered the de-
706 mand fulfillment decisions. However, both the fleet deployment and the demand ful-
707 fillment decisions are strategic in nature and are intertwined. This study proposed an
708 integrated decision model for optimizing the ship fleet deployment, the scheduling of
709 ship visits at each port of call, and the demand fulfillment scale for each OD pair. The
710 objective was to maximize the total benefit of shipping liners by considering various

711 types of operation costs for running shipping networks.

712 (2) The overload risk of transported containers has seldom been considered in
713 the FDP related literature, but this issue should not be ignored given the stochastic
714 weights of containers. Our study takes stochasticity into account by embedding chance
715 constraints in the decision model so as to control the overload risk under a certain
716 threshold probability. Some tactics were also suggested to handle the model's non-
717 linearity as well the complexity yielded by the chance constraints.

718 (3) Several realistic factors ignored in previous studies were considered in our
719 decision model, but solving them proved to be difficult. We have developed two
720 algorithms to solve the proposed non-linear chance-constrained MIP on large-scale
721 instances. Experiments conducted on real-world data demonstrate that our method-
722 ology yields solutions with an optimality gap less than about 0.5%, and can solve
723 realistic instances with 19 ports and four routes within about one hour.

724 **Acknowledgment**

725 This work was supported by the National Natural Science Foundation of China [grant
726 numbers 71831008, 71671107, 71422007, 71701178] and the Canadian Natural Sci-
727 ences and Engineering Research Council [grant number 2015-06189]. Thanks are due
728 to the reviewers for their valuable comments.

729 **References**

730 Alharbi, A., Wang, S., Davy, P., 2015. Schedule design for sustainable container
731 supply chain networks with port time windows. *Advanced Engineering Informatics*
732 29 (3), 322–331.

733 Álvarez, J. F., 2009. Joint routing and deployment of a fleet of container vessels.
734 *Maritime Economics & Logistics* 11 (2), 186–208.

735 Andersson, H., Fagerholt, K., Hobbesland, K., 2015. Integrated maritime fleet de-
736 ployment and speed optimization: Case study from ro-ro shipping. *Computers &*
737 *Operations Research* 55, 233–240.

738 Aydin, N., Lee, H., Mansouri, S. A., 2017. Speed optimization and bunkering in liner

- 739 shipping in the presence of uncertain service times and time windows at ports.
740 European Journal of Operational Research 259 (1), 143–154.
- 741 Bell, M. G., Liu, X., Angeloudis, P., Fonzone, A., Hosseinloo, S. H., 2011. A
742 frequency-based maritime container assignment model. Transportation Research
743 Part B: Methodological 45 (8), 1152–1161.
- 744 Bell, M. G., Liu, X., Rioult, J., Angeloudis, P., 2013. A cost-based maritime container
745 assignment model. Transportation Research Part B: Methodological 58, 58–70.
- 746 Chen, C., Zeng, Q., Zhang, Z., 2012. An integrating scheduling model for mixed
747 cross-operation in container terminals. Transport 27 (4), 405–413.
- 748 Cho, S.-C., Perakis, A., 1996. Optimal liner fleet routeing strategies. Maritime Policy
749 and Management 23 (3), 249–259.
- 750 Christiansen, M., Fagerholt, K., Nygreen, B., Ronen, D., 2013. Ship routing and
751 scheduling in the new millennium. European Journal of Operational Research
752 228 (3), 467–483.
- 753 Christiansen, M., Fagerholt, K., Ronen, D., 2004. Ship routing and scheduling: Status
754 and perspectives. Transportation Science 38 (1), 1–18.
- 755 Cordeau, J.-F., Laporte, G., Legato, P., Moccia, L., 2005. Models and tabu search
756 heuristics for the berth-allocation problem. Transportation Science 39 (4), 526–538.
- 757 Fagerholt, K., Johnsen, T. A., Lindstad, H., 2009. Fleet deployment in liner shipping:
758 a case study. Maritime Policy and Management 36 (5), 397–409.
- 759 Fransoo, J. C., Lee, C.-Y., 2013. The critical role of ocean container transport in
760 global supply chain performance. Production and Operations Management 22 (2),
761 253–268.
- 762 Gelareh, S., Meng, Q., 2010. A novel modeling approach for the fleet deployment
763 problem within a short-term planning horizon. Transportation Research Part E:
764 Logistics and Transportation Review 46 (1), 76–89.

- 765 Glover, F., 1986. Future paths for integer programming and links to artificial intelli-
766 gence. *Computers & Operations Research* 13 (5), 533–549.
- 767 Jaramillo, D., Perakis, A. N., 1991. Fleet deployment optimization for liner shipping
768 part 2. implementation and results. *Maritime Policy and Management* 18 (4), 235–
769 262.
- 770 Jiang, X. J., Jin, J. G., 2017. A branch-and-price method for integrated yard crane
771 deployment and container allocation in transshipment yards. *Transportation Re-
772 search Part B: Methodological* 98, 62–75.
- 773 Liu, M., Lee, C.-Y., Zhang, Z., Chu, C., 2016. Bi-objective optimization for the
774 container terminal integrated planning. *Transportation Research Part B: Method-
775 ological* 93, 720–749.
- 776 Meng, Q., Du, Y., Wang, Y., 2016. Shipping log data based container ship fuel
777 efficiency modeling. *Transportation Research Part B: Methodological* 83, 207–229.
- 778 Meng, Q., Wang, S., 2012. Liner ship fleet deployment with week-dependent container
779 shipment demand. *European Journal of Operational Research* 222 (2), 241–252.
- 780 Meng, Q., Wang, S., Andersson, H., Thun, K., 2014. Containership routing and
781 scheduling in liner shipping: overview and future research directions. *Transporta-
782 tion Science* 48 (2), 265–280.
- 783 Meng, Q., Wang, T., 2010. A chance constrained programming model for short-term
784 liner ship fleet planning problems. *Maritime Policy and Management* 37 (4), 329–
785 346.
- 786 Meng, Q., Wang, T., 2011. A scenario-based dynamic programming model for multi-
787 period liner ship fleet planning. *Transportation Research Part E: Logistics and
788 Transportation Review* 47 (4), 401–413.
- 789 Meng, Q., Wang, T., Wang, S., 2012. Short-term liner ship fleet planning with con-
790 tainer transshipment and uncertain container shipment demand. *European Journal
791 of Operational Research* 223 (1), 96–105.

- 792 Monemi, R. N., Gelareh, S., 2017. Network design, fleet deployment and empty repositioning in liner shipping. *Transportation Research Part E: Logistics and Transportation Review* 108, 60–79.
- 793
794
- 795 Nikolopoulou, A. I., Repoussis, P. P., Tarantilis, C. D., Zachariadis, E. E., 2017. Moving products between location pairs: Cross-docking versus direct-shipping. *European Journal of Operational Research* 256 (3), 803–819.
- 796
797
- 798 Perakis, A. N., Jaramillo, D., 1991. Fleet deployment optimization for liner shipping part 1. background, problem formulation and solution approaches. *Maritime Policy and Management* 18 (3), 183–200.
- 799
800
- 801 Petering, M. E., Wu, Y., Li, W., Goh, M., de Souza, R., Murty, K. G., 2017. Real-time container storage location assignment at a seaport container transshipment terminal: dispersion levels, yard templates, and sensitivity analyses. *Flexible Services and Manufacturing Journal* 29 (3–4), 369–402.
- 802
803
804
- 805 Powell, B., Perkins, A., 1997. Fleet deployment optimization for liner shipping: An integer programming model. *Maritime Policy and Management* 24 (2), 183–192.
- 806
- 807 Qi, X., Song, D.-P., 2012. Minimizing fuel emissions by optimizing vessel schedules in liner shipping with uncertain port times. *Transportation Research Part E: Logistics and Transportation Review* 48 (4), 863–880.
- 808
809
- 810 Ronen, D., 1993. Ship scheduling: The last decade. *European Journal of Operational Research* 71 (3), 325–333.
- 811
- 812 Tirado, G., Hvattum, L. M., Fagerholt, K., Cordeau, J.-F., 2013. Heuristics for dynamic and stochastic routing in industrial shipping. *Computers & Operations Research* 40 (1), 253–263.
- 813
814
- 815 Vivaldini, K., Rocha, L. F., Martarelli, N. J., Becker, M., Moreira, A. P., 2016. Integrated tasks assignment and routing for the estimation of the optimal number of agvs. *The International Journal of Advanced Manufacturing Technology* 82 (1–4), 719–736.
- 816
817
818

- 819 Wang, C., Xu, C., 2015. Sailing speed optimization in voyage chartering ship consid-
820 ering different carbon emissions taxation. *Computers & Industrial Engineering* 89,
821 108–115.
- 822 Wang, H., Zhang, X., Wang, S., 2016. A joint optimization model for liner contain-
823 er cargo assignment problem using state-augmented shipping network framework.
824 *Transportation Research Part C: Emerging Technologies* 68, 425–446.
- 825 Wang, S., Meng, Q., 2012. Liner ship fleet deployment with container transshipment
826 operations. *Transportation Research Part E: Logistics and Transportation Review*
827 48 (2), 470–484.
- 828 Wang, S., Meng, Q., 2015. Robust bunker management for liner shipping networks.
829 *European Journal of Operational Research* 243 (3), 789–797.
- 830 Wang, S., Meng, Q., Liu, Z., 2013. Bunker consumption optimization methods in
831 shipping: A critical review and extensions. *Transportation Research Part E: Lo-*
832 *gistics and Transportation Review* 53, 49–62.
- 833 Wang, S., Wang, T., Meng, Q., 2011. A note on liner ship fleet deployment. *Flexible*
834 *Services and Manufacturing Journal* 23 (4), 422–430.
- 835 Wang, T., Meng, Q., Wang, S., 2012. Robust optimization model for liner ship fleet
836 planning with container transshipment and uncertain demand. *Transportation Re-*
837 *search Record: Journal of the Transportation Research Board* (2273), 18–28.
- 838 Wang, X., Fagerholt, K., Wallace, S. W., 2017. Planning for charters: A s-
839 tochastic maritime fleet composition and deployment problem. *Omega*, DOI
840 10.1016/j.omega.2017.07.007.
- 841 Wang, Y., Meng, Q., Du, Y., 2015. Liner container seasonal shipping revenue man-
842 agement. *Transportation Research Part B: Methodological* 82, 141–161.
- 843 Wen, M., Pacino, D., Kontovas, C. A., Psaraftis, H. N., 2017. A multiple ship routing
844 and speed optimization problem under time, cost and environmental objectives.
845 *Transportation Research Part D: Transport and Environment* 52, 303–321.

- 846 Xia, J., Li, K. X., Ma, H., Xu, Z., 2015. Joint planning of fleet deployment, speed
847 optimization, and cargo allocation for liner shipping. *Transportation Science* 49 (4),
848 922–938.
- 849 Yao, Z., Ng, S. H., Lee, L. H., 2012. A study on bunker fuel management for the
850 shipping liner services. *Computers & Operations Research* 39 (5), 1160–1172.
- 851 Yi, W., Chi, H.-L., Wang, S., 2018. Mathematical programming models for construc-
852 tion site layout problems. *Automation in Construction* 85, 241–248.
- 853 Zacharioudakis, P. G., Iordanis, S., Lyridis, D. V., Psaraftis, H. N., 2011. Liner
854 shipping cycle cost modelling, fleet deployment optimization and what-if analysis.
855 *Maritime Economics & Logistics* 13 (3), 278–297.
- 856 Zhao, Y., Jia, R., Jin, N., He, Y., 2016. A novel method of fleet deployment based
857 on route risk evaluation. *Information Sciences* 372, 731–744.
- 858 Zhen, L., 2015. Tactical berth allocation under uncertainty. *European Journal of*
859 *Operational Research* 247 (3), 928–944.
- 860 Zhen, L., 2016. Modeling of yard congestion and optimization of yard template in
861 container ports. *Transportation Research Part B: Methodological* 90, 83–104.
- 862 Zheng, J., Gao, Z., Yang, D., Sun, Z., 2015. Network design and capacity exchange for
863 liner alliances with fixed and variable container demands. *Transportation Science*
864 49 (4), 886–899.